UCRL 13662

TRANSIENT COMPRESSIBLE FLOWS IN POROUS MEDIA

Frank A. Morrison, Jr.
Department of Mechanical and Industrial Engineering
University of Illinois at Urbana-Champaign
Urbana, IL 61801

Final Report (UILU ENG 75 4004)
of Research Performed under
Subcontract No. 1160305
for
THE REGENTS OF THE UNIVERSITY OF CALIFORNIA

September 1975

Copy No. 2 of Ten (10) Copies

TRANSIENT COMPRESSIBLE FLOWS IN POROUS MEDIA

Frank A. Morrison, Jr.

Department of Mechanical and Industrial Engineering
University of Illinois at Urbana-Champaign
Urbana, IL 61801

Final Report (UILU ENG 75 4004)
of Research Performed under
Subcontract No. 7160305
for
THE REGENTS OF THE UNIVERSITY OF CALIFORNIA

September 1975

FOREWORD

This research was supported by the Lawrence Livermore Laboratory under Subcontract No. 1160352 of Contract No. W-7405-Eng 48. Technical coordinator was J. H. Pitts. Contract administrator was E. I. Halonen.

Dr. F. A. Morrison, Jr., Professor of Mechanical Engineering, acted as principal investigator. In addition, J. H. Johnson, R. S. Downing, and M. B. Stewart participated in the investigation.

ABSTRACT

Transient compressible flow in porous media has been investigated analytically. The major portion of the investigation has been directed toward improving the understanding of dispersion in these flows and developing rapid accurate numerical techniques for predicting the extent of dispersion. The results are of interest in the containment of underground nuclear experiments.

The transport of matter in porous media consists of convective and dispersive transport. Convective transport is an ordered motion at some mean local fluid velocity. Purely convective transport is a piston-like flow where the invading fluid completely displaces the fluid initially within a pore. A dispersive flow results from random disordered phenomena such as mixing and molecular diffusivity. The two types of transport are both important in the flows considered here.

Dispersive transport may be described by a dispersion coefficient similar in effect to a diffusion coefficient. At low Peclet numbers, dispersion results primarily from molecular diffusion and the dispersion coefficient is of the order of magnitude of the molecular diffusivity. At high Peclet numbers, the dispersion coefficient is dependent on the local Peclet number and is roughly proportional to it.

The transient one-dimensional transport of a trace component in a gas flow is analyzed. A conservation equation for mass for the effects of convective transport, dispersive transport, and decay, is developed. This relation, as well as a relation governing the fluid flow, is used to predict trace component concentration as a function of position and time.

A detailed analysis of transport associated with the isothermal flow of an ideal gas is done. Because the governing equations are nonlinear,

numerical calculations are performed. The ideal gas flow is calculated using a highly stable implicit iterative procedure with an Eulerian mesh. In order to avoid problems of anomalous dispersion associated with finite-difference calculation, trace component convection and dispersion are calculated using a Lagrangian mesh.

Details of the Eulerian-Lagrangian numerical technique are presented. Computer codes have been developed and implemented on the Lawrence Livermore Laboratory computer system.

TABLE OF CONTENTS

INTRODUCTION

Following an underground nuclear experiment, cavity gas may enter the surrounding porous material or the existing rubble. The high pressure existing within the cavity serves to drive this fluid through the porous medium. This flow may continue for several minutes until cavity collapse when the driving pressure decreases significantly. Containment evaluation includes a determination of the extent of cavity gas penetration.

Previous analyses [1,2]* of the flow resulting from an explosive test have determined the extent of penetration by assuming a piston like displacement. The gas issuing from the cavity is presumed not to mix with the gas originally present, but to totally displace it. The actual mechanism, of course, involves some mixing. A purpose of this investigation is to determine the extent of this mixing and to establish the utility of the piston flow approximation.

ANALYSIS AND RESULTS

Theory and experiment indicate that dispersion in porous media can quite accurately be described by a Fick's law-type expression, that is, *a relation such as gaseous diffusion. For a one-dimensional* flow, such as we examine here, the dispersive flux of a trace specie is given by

$$J_D = -D \frac{\partial c}{\partial x}$$

c is the concentration, x is the position coordinate in the direction of *transport, and D is the dispersion coefficient.* Much study has been directed toward predicting the value of the dispersion coefficient. It is clear, however, that dispersivities correlations based on experiment *are currently the most dependable source of dispersion coefficients.* Perkins and Johnston [5] review some of the early work on dispersion coefficients. A more recent survey may be found in Bear [1].

The salient features of dispersion in porous media can be described quite simply. Dispersion results from molecular diffusivity and from a convective dispersion resulting from fluid motion. The relative importance of the two effects depends on the local Peclet number of the flow.

The Peclet number (NPE) is the product of the Schmidt number (NSC) and the Reynolds number (NRY). The Peclet number is *a ratio expressing* the relative significance of convective transport and transport resulting *from molecular diffusion.* The appropriate length scale, d, is a pore or grain size; v is the apparent fluid velocity; and D and ν are molecular diffusivity *and kinematic viscosity,* respectively.

The Schmidt number depends only on fluid properties and, for gases, is typically of order unity. *The Peclet number, then, varies primarily* with Reynolds number and has a value of the order of the Reynolds number. The character of the transport is governed by the Reynolds number.

For low Reynolds number (low Peclet number) flow, the dispersion results primarily from molecular diffusion. The dispersion coefficient differs from the diffusion coefficient only by a small geometric factor for the tortuosities of the paths. Variation in the dispersion coefficient results primarily from variation in the diffusion coefficient. Molecular diffusivity depends on both temperature and pressure. However, since gas flow through porous media is normally isothermal, only the pressure dependence is significant. In low Peclet number, dispersion is described by a dispersion coefficient that is independent of flow rate and varies inversely with the local pressure

$$D = D_0 \frac{P_0}{P},$$

D is dispersivity and P is the local pressure.

Low Reynolds number convective dispersive transport can be analyzed using this description of dispersion. Numerical techniques have been developed for the calculation of such transport. Because of the very large numerical dispersion generated by normal finite-element techniques, an Eulerian-Lagrangian method was developed. A description of this method was presented at the CBMF Symposium [3] and appears in this report as APPENDIX A.

A more detailed analysis of low Reynolds number transport has been prepared and appears as APPENDIX B. The equations governing this transport are derived. The Eulerian-Lagrangian technique is developed. Results of calculations are presented for transport resulting from a step change of an isothermal ideal gas through a uniform porous bed.

Following the formulation and analysis of low Reynolds number transport, attention was directed at higher Reynolds number flows. The origin

of the interest is the dependence of the dispersion coefficient on Reynolds number. While the dispersion coefficient is reasonably constant for Reynolds numbers less than about one, the coefficient steadily increases with further increases in Reynolds number. This dependence is apparently linear in a porous bed.

In order to investigate the effect of higher Reynolds number on transport, it was necessary to first develop an algorithm for calculating the velocity and pressure distribution of the carrier gas.

At low Reynolds numbers, less than 0.1, the apparent fluid velocity is proportional to the local pressure gradient, obeying Darcy's law.

$$u = -\frac{k}{\mu}\frac{\partial p}{\partial x}$$

k is the permeability, a property of the solid medium. μ is the fluid viscosity. At higher Reynolds numbers, inertial effects become significant and Darcy's law ceases to be a satisfactory description of the flow. Instead, empirical constitutive equations accounting for inertial influences are employed. Of these, Forchheimer's [o] relation

$$u + b_1 [u] u = -\frac{k}{\mu}\frac{\partial p}{\partial x}$$

is at once one of the oldest relations, has considerable experimental justification, and a broad range of applicability. Forchheimer's relation modifies Darcy's law by the addition of a second-order term in velocity. ρ is the gas density and b is a constant depending on the structure of the medium and fluid viscosity.

A more detailed description of high Reynolds number flow is presented in APPENDIX C. Flow in finite and infinite beds is analyzed. A similarity analysis is presented. A numerical technique is developed to describe these flows. Results of calculations show the behavior of high

Reynolds number flows. The Reynolds number used to characterize these flows is

$$Re = \frac{\rho_0 k(p_1 - p_0) b}{\mu L}$$

This is roughly a Reynolds number based on local velocity, local velocity and a pore dimension.

Having described the notion of the variable permeability flow system, it remains to describe the dispersion relation. A linear relationship between dispersivity and Peclet number was employed, extending the form used for low Reynolds numbers.

$$\mathcal{D} = \mathcal{D}_0 \frac{\rho_0}{\rho} (1 + 1.75 Pe)$$

The factor of 1.75 is applicable to a typical random packing [3]. The Peclet number is here defined by

$$Pe = \frac{u\, d}{\mathcal{D}_0\, \rho_0/\rho}$$

d is a typical pore dimension. Because of variations in local pressure and velocity, the Peclet number is not constant for a particular flow.

In order to characterize the additional contribution to dispersion by a single constant, we use the dimensionless velocity defined in APPENDIX B and APPENDIX C.

$$U = \frac{u\, L\, \mu}{k(p_1 - p_0)}$$

and a dimensionless diffusivity defined in APPENDIX B.

$$D = \frac{\mu\, \mathcal{D}\, \rho_0/\rho}{k(p_1 - p_0)}.$$

In terms of these variables, we have

$$Pe = \frac{U}{D} \frac{d}{L}.$$

The ratio (d/L) of pore diameter to bed length is [illegible] small [illegible] related to [illegible]. [illegible] the effect of [illegible] on dispersion [illegible] negligible in such [illegible].

An [illegible] was [illegible] in order to [illegible] the effect of [illegible] dispersion [illegible] calculations [illegible] effect [illegible] Reynolds number.

Consider the transport [illegible] by a Reynolds number [illegible] ratio of [illegible] transient pressure distribution [illegible] step pressure [illegible] shown in Fig. 1. [illegible] APPENDIX [illegible] the [illegible] Reynolds number effects [illegible] concentration distribution. Figure 2 [illegible] convective transport [illegible] propagation rate differs significantly from [illegible] for the [illegible] shown in Fig. 2, of APPENDIX [illegible].

Effects of dispersion are shown in the final two figures. Figure [illegible] shows dispersion varying [illegible] only with pressure. [illegible] on Peclet number is revealed by the increased dispersion [illegible] in Fig. [illegible]. In this case, d/L is 10^{-2} corresponding to a bed length of [illegible] meters. When this effect is included, local dispersion [illegible] larger in regions of high pressure and high velocity. Dispersion [illegible] considerably enhanced. The effect, however, is significant only for [illegible] times or short beds.

DISCUSSION

Convective-dispersive transport in compressible gas flow has been investigated analytically. The governing relations describing this transport have been formulated. Numerical procedures have been developed to accurately calculate transport and to calculate high Reynolds number gas flow. Results of such calculations have been presented and discussed.

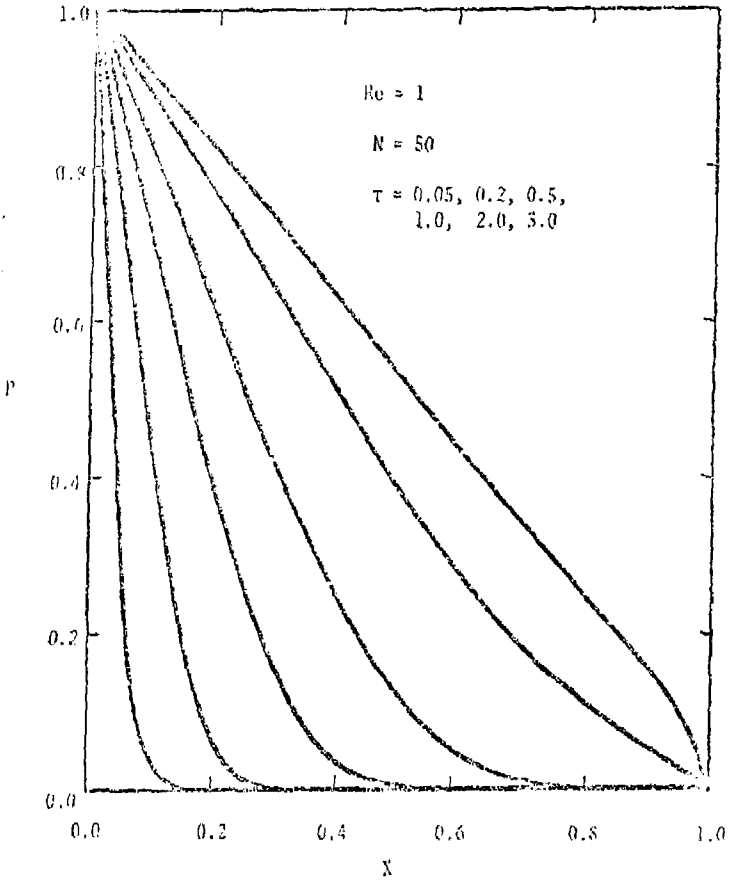

Figure 1

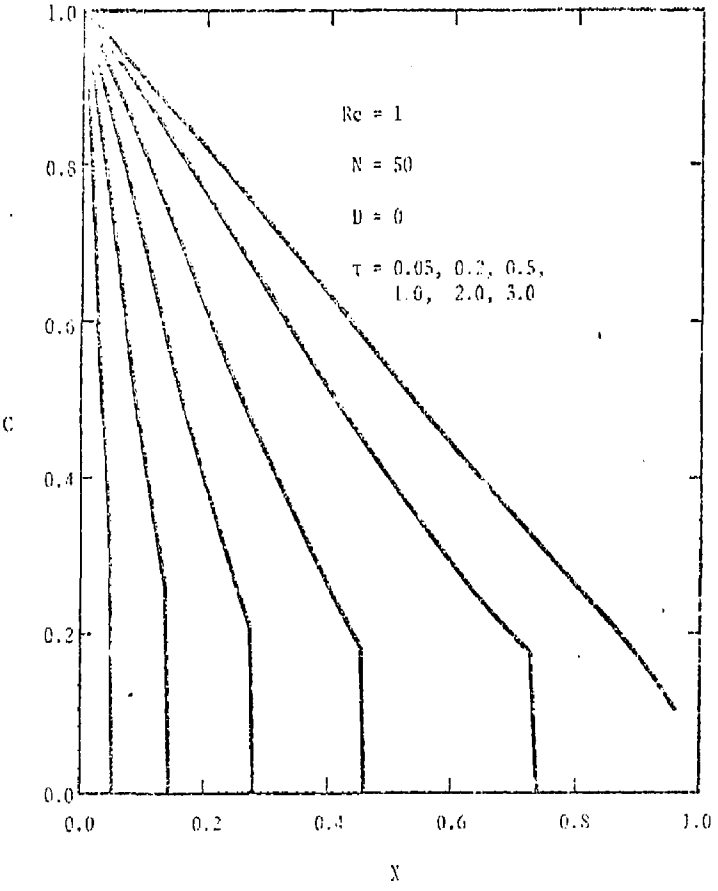

Figure 2

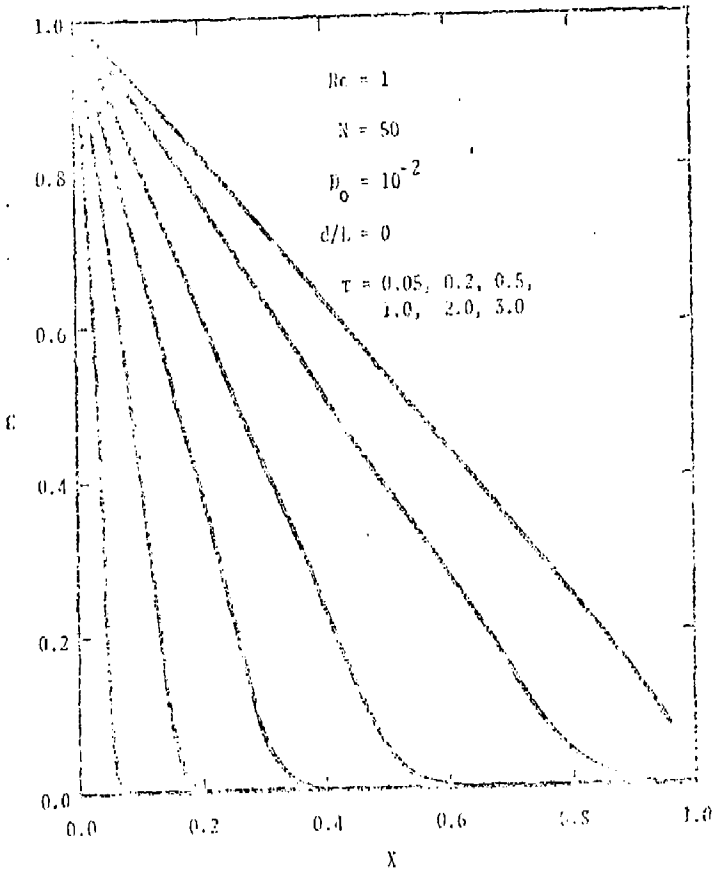

Figure 5

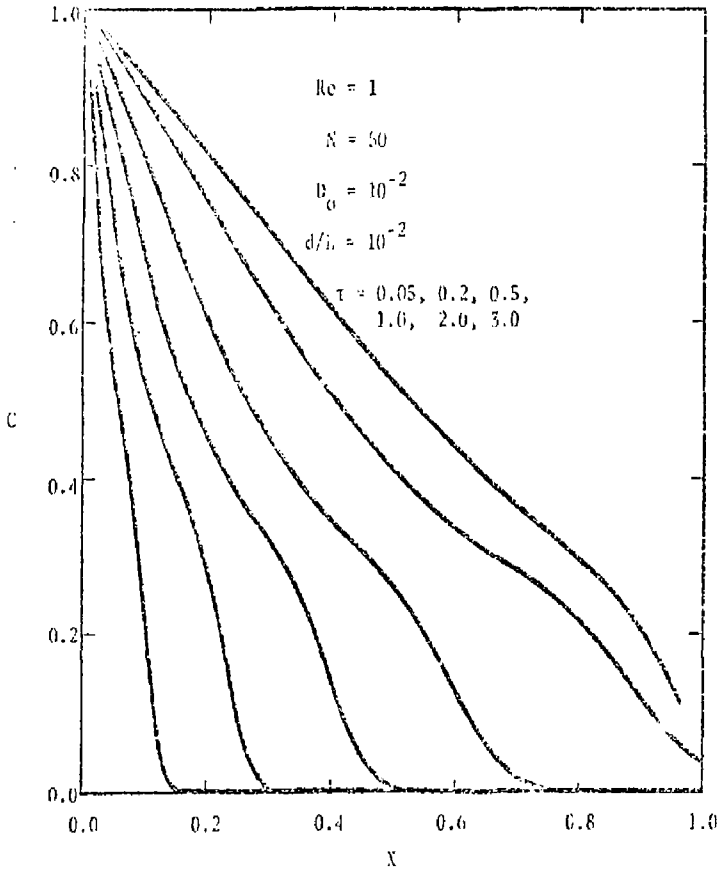

Figure 3

REFERENCES

1. F. A. Morrison, Jr., Transient gas flow in a porous column, Ind. Eng. Chem. Fund. 11, 191 (1972).

2. F. A. Morrison, Jr., Transient multiphase multicomponent flow in porous media, Int. J. Heat Mass Transfer 16, 2351 (1973).

3. T. K. Perkins and O. C. Johnston, A review of diffusion and dispersion in porous media, Trans. Am. Inst. Min. Engrs. 228, 70 (1963).

4. J. Bear, Dynamics of fluids in porous media, American Elsevier, New York (1972).

5. F. A. Morrison, Jr., An Eulerian-Lagrangian method for convective-dispersive transport, Proc. CUBE Symp., 225 (1974) (CONF-741001).

6. Ph. Forchheimer, Wasserbewegung durch Boden, Zeitschrift des Vereines Deutscher Ingenieure 45, 1781 (1901).

APPENDIX A

AN EULERIAN-LAGRANGIAN METHOD FOR CONVECTIVE-DISPERSIVE TRANSPORT

Frank A. Morrison, Jr.

AN EULERIAN-LAGRANGIAN METHOD FOR CONVECTIVE-DISPERSIVE TRANSPORT

Frank A. Morrison, Jr.
Lawrence Livermore Laboratory
Professor of Mechanical Engineering
University of Illinois at Urbana-Champaign
Urbana, IL 61801

ABSTRACT

Convective-dispersive transport in a one-dimensional compressible flow is solved using an Eulerian-Lagrangian technique. The transport of a tagged species, resulting from dispersion and gas flow in porous media, is studied. The velocity distribution of the bulk gas motion is calculated using an Eulerian viewpoint. This velocity distribution determines the motion of the Lagrangian mesh. The mixed Eulerian-Lagrangian approach is adopted as a means of avoiding anomolous numerical dispersion. A Lagrangian mesh moves along characteristic curves of the convective transport equation. Any transport relative to this mesh is dispersive. In the absence of physical dispersion, there is no transfer of the species between Lagrangian mesh points and concentration changes then result solely from compression and expansion of the fluid element. Because the flow is compressible, the Lagrangian mesh points are unequally spaced. Implicit methods for solution of the diffusion equation are developed for unequally spaced mesh points. Detailed calculations have been done for the transient, low Reynolds number, isothermal flow of an ideal gas.

INTRODUCTION

Convective and dispersive transport are associated with many processes of engineering significance. Techniques developed for the analysis of the relations governing these phenomena may, consequently, have wide applicability. Here, we present some techniques developed in the analysis of miscible displacement in a transient compressible flow through porous media. Because the relation governing the bulk fluid velocity distribution is nonlinear, numerical techniques are used. We examine difficulties encountered in the numerical solution of the convective-dispersive transport equation and describe means of overcoming these difficulties.

We consider the transport in one space dimension of a trace component characterized by a concentration c. c is a function of position x and time t. The concentration distribution is to be determined. The governing relation is obtained simply by applying conservation of species to an infinitesimal element of space. The convective flux across a unit control surface normal to the direction of flow is uc. u is the apparent velocity, volume flow rate per unit normal area, of the carrier gas. The dispersive transport is normally considered, like diffusion, to obey a relation of the form of Fick's law. Using a dispersion coefficient, D, the flux is $-D(\partial c/\partial x)$. Equating the net flux into the element to the rate of accumulation within the element, the transport equation results.

$$\varepsilon \frac{\partial c}{\partial t} + \frac{\partial}{\partial x}\left(uc - D\frac{\partial c}{\partial x}\right) = 0 \qquad (1)$$

ε is the porosity of the medium, the void volume fraction.

In an incompressible flow in one dimension, the velocity u is constant. Additionally, the dispersivity is often taken to be constant. Neither simplification is valid in our application. The equation governing the concentration distribution has nonconstant coefficients, u and D, functions of position and time and determined by numerical techniques. The velocity and dispersivity result from solution of the equation governing bulk gas motion.

MOTION OF THE FLUID

The form in which the fluid velocity distribution becomes known affects the subsequent choice of tools utilizing this distribution.

The low Reynolds number flow of an isothermal ideal gas in one dimension

obeys a well known[1,2] relation

$$\frac{\partial}{\partial x}\left(p\,\frac{\partial p}{\partial x}\right) = \frac{\epsilon\mu}{k}\frac{\partial p}{\partial t} \qquad (2)$$

p is the local gas pressure, while μ is the gas viscosity and k, the permeability of the medium. The gas velocity is expressed in terms of the pressure gradient by Darcy's law.

$$u = -\frac{k}{\mu}\frac{\partial p}{\partial x} \qquad (3)$$

The dispersion coefficient is independent of velocity in the low Reynolds number, low Peclet number range. It does, however, vary inversely with the gas pressure

$$D = D_o\frac{p_o}{p} \qquad (4)$$

The subscript o refers to ambient conditions. Calculation of the pressure distribution yields the velocity and dispersivity distributions.

Equation (2) is analogous to a nonlinear heat conduction equation. The numerical procedure chosen for its solution is the method of Bruce, Peaceman, Rachford, and Rice.[3] This is an implicit, unconditionally stable procedure similar to the Crank-Nicolson[4] method for the linear diffusion equation. Because of the nonlinearity of Eq. (2), the procedure is iterative. However, the convergence is rapid. Moreover, the coefficient matrix of the finite difference equations is tridiagonal so that each iteration is efficiently performed using Thomas'[5] algorithm.

NUMERICAL DISPERSION

Because an Eulerian approach is used to determine the velocity and dispersivity distributions, Eulerian methods should be considered for subsequent analysis of the trace component transport. Eulerian techniques, however, tend to produce an anomolous numerical dispersion which could easily exceed the physical dispersion of interest.

Consider, as an example, convective transport in an incompressible flow. In this simple case, Eq. (2) reduces to

$$\epsilon\frac{\partial c}{\partial t} + u\frac{\partial c}{\partial x} = 0 \qquad (5)$$

having

$$x = x_o + \frac{u}{\epsilon}t \qquad (6)$$

as a characteristic curve. c is constant on a characteristic. There is no physical dispersion. Now, consider a finite difference approximation to Eq. (5).

$$\epsilon\frac{c_i^{k+1} - c_i^k}{\Delta t} + u\frac{c_i^k - c_{i-1}^k}{\Delta x} = 0 \qquad (7)$$

The expression is chosen to employ upwind differencing. The superscripts refer to the time level while the subscripts are spatial indices. Using Taylor series expansions for the concentration, we may readily show that Eq. (7) is equivalent to

$$\epsilon\frac{\partial c}{\partial t} + u\frac{\partial c}{\partial x} = \frac{u\Delta x}{2}\left(1 - \frac{u\Delta t}{\epsilon\Delta x}\right)\frac{\partial^2 c}{\partial x^2} + \cdots \qquad (8)$$

The coefficient of the second spatial derivative on the right side is a numerical dispersion coefficient. It results from the use of the finite difference expression. This coefficient can exceed the actual dispersion coefficient by orders of magnitude.

Because the flow actually being considered is compressible, the situation is even more complex. The velocity varies with position and time. Techniques developed to eliminate artificial dispersion in Eulerian calculations, but relying on a uniform fluid velocity, are not applicable. Accordingly, a mixed Eulerian-Lagrangian approach was considered and then adopted. In addition to the fixed Eulerian grid used to calculate p, u, and D, a moving Lagrangian mesh is used to determine the concentration, c.

A Lagrangian observer moves, with a fluid element, along a characteristic curve of the convective transport equation. The velocity of a Lagrangian mesh point is

$$\frac{dx}{dt} = \frac{u}{\epsilon} \qquad (9)$$

There is no convective transport

between Lagrangian mesh points. Such transport occurs solely as a result of dispersion. The numerical dispersion of the Eulerian approach resulted from the convective transport through the Eulerian mesh. When a Lagrangian viewpoint is adopted, there is no such transport and no numerical mechanism producing such transport is generated. The Lagrangian approach provides a natural means of eliminating artificial dispersion, valid for compressible flow and for flow with physical dispersion. A Lagrangian technique has been used by Garder, Peaceman, and Pozzi[4] to treat dispersion in an incompressible flow through porous media. The technique described here differs by including compressibility and also differs in the means of calculating dispersive transport.

LAGRANGIAN FORMULATION

A temporal derivative in the Lagrangian frame is expressed by the material or substantial derivative.

$$\frac{d}{dt} = \frac{\partial}{\partial t} + \frac{u}{\varepsilon}\frac{\partial}{\partial x} \qquad (10)$$

so that the convective-dispersive transport equation, Eq. (2), becomes

$$\varepsilon \frac{dc}{dt} + c\frac{\partial u}{\partial x} = \frac{\partial}{\partial x}\left(D\frac{\partial c}{\partial x}\right) \qquad (11)$$

The first term on the left side of Eq. (11) is the rate of change of concentration in a fluid element. This results from dispersion, expressed on the right side, but also from compression or expansion of the fluid element as expressed in the second term on the left.

As a result of this compressibility, the concentration is not constant on a characteristic curve even in the absence of dispersion. Additionally, the spacing between successive Lagrangian mesh points will vary as they move through the medium. Neither of these effects are present in an incompressible flow.

CONVECTIVE TRANSPORT

First, let us address the problem of calculating the positions of the points in the nonuniform expanding Lagrangian mesh. The instantaneous velocity of any Lagrangian mesh point, ℓ, is given by Eq. (9). The velocity, u, is given in terms of the pressure gradient by Eq. (3). The problem reduces to one of interpolating to obtain the pressure gradient at the location of ℓ. The pressure is known at each of the Eulerian nodes. These Eulerian nodes are separated by a distance Δx. The Lagrangian node, ℓ, is a distance, $f\Delta x$, in front of the nearest Eulerian node, i.

$$|f| \leq 1/2 \qquad (12)$$

The pressures at the Eulerian nodes, $i-1$, i, and $i+1$, can be expressed in terms of a Taylor series expansion about ℓ. These three expressions are then solved to yield the pressure gradient, and thus the velocity, at the Lagrangian node.

$$\left.\frac{\partial p}{\partial x}\right|_{\ell} = \frac{(2f+1)p_{i+1} - 4fp_i + (2f-1)p_{i-1}}{2\Delta x} + \frac{1-3f^2}{6}\Delta x^2 \left.\frac{\partial^3 p}{\partial x^3}\right|_{\ell} + \cdots \qquad (13)$$

Numerical integration of velocity yields the node position as a function of time. Because the local velocity changes with position and time, however, the node velocity during a time interval Δt is better approximated by a mean of calculated velocities at the two time levels and at the new and old positions. The new position is unknown, however, until the calculation is complete. An iterative procedure to determine the new position is employed. A single iteration appears to be adequate in our application. Such time centering of Lagrangian node motion calculations has previously been proposed by Forester.[7]

The concentration changes resulting from expansion of a fluid element may now be treated. This contribution to the variation of concentration is described by Eq. (11) with dispersivity set equal to zero.

$$\varepsilon \frac{dc}{dt} + c\frac{\partial u}{\partial x} = 0 \qquad (14)$$

The velocity gradient, $\partial u/\partial x$, is positive in an expanding flow and negative in a compressing flow. It can be calculated by a variety of methods. The method recommended here, however, is to eliminate the calculation entirely with the following observation.

The bulk fluid density obeys a convective transport equation analogous to Eq. (14). This is the continuity

equation.

$$\varepsilon \frac{d\rho}{dt} + \rho \frac{\partial u}{\partial x} = 0 \qquad (15)$$

Consequently, the concentration of a fluid element changes in proportion with the density. Because the density in an isothermal ideal gas is proportional to the pressure, the concentration becomes proportional to the pressure of the fluid element.

Because of dispersivity in the general case, the concentration does not remain proportional to the pressure. Instead, the concentration change for a single time step is separated into convective and dispersive changes. Starting with the concentration, c_ℓ^k, of the ℓth Lagrangian node at time level k, the convective contribution yields an intermediate value of the new concentration.

$$c_\ell^{k+1} = c_\ell^k \frac{P_\ell^{k+1}}{P_\ell^k} \qquad (16)$$

The intermediate spatial distribution of concentration is then used to determine how dispersion affects the concentration distribution at this time level. Note that, without explicitly introducing dispersion, no dispersion is generated.

The pressure used in Eq. (16) is found by a procedure similar to that used to obtain Eq. (13), the pressure gradient interpolation.

$$P_\ell = \frac{f(f+1)}{2} P_{i+1} + (1 - f^2) P_i + \frac{f(f-1)}{2} P_{i-1} - \frac{1}{6} f(1 - f^2) \Delta x^3 \left.\frac{d^3 p}{dx^3}\right|_\ell + \cdots \qquad (17)$$

Having accounted for node movement, expansion, and compression, it remains to calculate the dispersive contribution to transport of the tagged species.

DISPERSIVE TRANSPORT

Dispersive transport is governed by Eq. (11) with the fluid velocity set equal to zero.

$$\varepsilon \frac{dc}{dt} = \frac{\partial}{\partial x}\left(D \frac{\partial c}{\partial x}\right) \qquad (18)$$

This is the diffusion equation. Its solution here is complicated only by the fact that the Lagrangian mesh is nonuniform.

In order to find the concentrations at time level $k + 1$, the Lagrangian grid is held in its $k + 1$ configuration. The intermediate concentrations, calculated to account for expansion and described in the previous section, are treated as the concentrations at time level k but in the new positions. The order of operations is as if the node movement and fluid expansion occurs instantaneously, then the tagged species disperses through stationary fluid for a period of time Δt.

The finite difference approximation to Eq. (18) is developed in an analogous form to techniques widely used in the solution with a uniform mesh. For a uniform mesh, one would write

$$\varepsilon \frac{c_\ell^{k+1} - c_\ell^k}{\Delta t} = \frac{\beta[\delta(D\delta c)]^{k+1} + (1 - \beta)[\delta(D\delta c)]^k}{\Delta x^2} \qquad (19)$$

δ is the central difference operator. β is a factor weighting the calculation of the second spatial derivative between time levels k and $k + 1$.

β is zero for an explicit calculation. If β is 1/2 and D is constant, this is the Crank-Nicolson method. For $\beta \geq 1/2$, the calculation is unconditionally stable. Note that the coefficient matrix of the unknown concentrations is tridiagonal, so that the same efficient algorithm as was employed to calculate pressure could be used here.

When treating the nonuniform mesh, it is desirable to retain a tridiagonal form because of the considerable savings in computational time. There is a penalty in accuracy however. A three-point approximation to the second derivative, for example, has a lower order error than the uniform mesh equivalent.

$$\left.\frac{\partial^2 c}{\partial x^2}\right|_\ell = \frac{2c_{\ell+1}}{(x_{\ell+1} - x_\ell)(x_{\ell+1} - x_{\ell-1})}$$

$$- \frac{2c_\ell}{(x_{\ell+1} - x_\ell)(x_\ell - x_{\ell-1})}$$

$$+ \frac{2c_{\ell-1}}{(x_\ell - x_{\ell-1})(x_{\ell+1} - x_{\ell-1})}$$

$$- \frac{1}{3}(x_{\ell+1} - 2x_\ell + x_{\ell-1})$$

$$\cdot \left.\frac{\partial^3 c}{\partial x^3}\right|_\ell + \cdots \qquad (20)$$

The leading error term vanishes for a uniform mesh. A nonuniform mesh should be generated so as to maintain small values for these additional error terms. A smooth slow variation of mesh size is best from this standpoint.

With varying diffusivity, the nonuniform mesh equivalent of Eq. (19) was taken as

$$\varepsilon \frac{c_\ell^{k+1} - c_\ell^k}{\Delta t} = \frac{2\beta}{x_{\ell+1} - x_{\ell-1}} \left(D_{\ell+\frac{1}{2}} \frac{c_{\ell+1} - c_\ell}{x_{\ell+1} - x_\ell} - D_{\ell-\frac{1}{2}} \frac{c_\ell - c_{\ell-1}}{x_\ell - x_{\ell-1}} \right)^{k+1}$$

$$+ \frac{2(1-\beta)}{x_{\ell+1} - x_{\ell-1}} \cdot \left(D_{\ell+\frac{1}{2}} \frac{c_{\ell+1} - c_\ell}{x_{\ell+1} - x_\ell} - D_{\ell-\frac{1}{2}} \frac{c_\ell - c_{\ell-1}}{x_\ell - x_{\ell-1}} \right)^{k} \qquad (21)$$

For β equal to 1/2, a slight oscillation was observed in the results. A weighting factor, β, greater than 1/2 is recommended. No oscillation appears for larger β.

CONCLUSIONS

The numerical treatment of convective and dispersive transport has been considered. Reasons for utilizing an Eulerian-Lagrangian approach have been presented. Techniques for accurately determining mesh movement, fluid expansion, and trace element dispersion are described. These techniques have been developed for the analysis of transport associated with gas flows in porous media. A program, *DIASPORA*, employing these methods has been written and implemented on the CDC 7600s at the Lawrence Livermore Laboratory.

REFERENCES

[1] A. E. Scheidegger, The Physics of Flow through Porous Media (MacMillan, New York, 1960)

[2] F. A. Morrison, Jr., I. & E. C. Fund. 11, 191 (1972)

[3] G. H. Bruce, D. W. Peaceman, H. H. Rachford, Jr., and J. D. Rice, Pet. Trans. AIME 198, 79 (1953)

[4] J. Crank and P. Nicolson, Proc. Camb. Phil. Soc. 43, 50 (1947)

[5] D. U. von Rosenberg, *Methods for the Numerical Solution of Partial Differential Equations* (American Elsevier, New York, 1969)

[6] A. O. Carder, Jr., D. W. Peaceman, and A. L. Pozzi, Jr., Pet. Trans. AIME 231, 26 (1964)

[7] C. K. Forester, J. Computational Phys. 12, 269 (1973)

APPENDIX B

CONVECTIVE AND DISPERSIVE TRANSPORT IN A POROUS MEDIUM

R. S. Downing

F. A. Morrison, Jr.

CONVECTIVE AND DISPERSIVE TRANSPORT IN A POROUS MEDIUM*

R. S. Downing

F. A. Morrison, Jr.

Department of Mechanical and Industrial Engineering
University of Illinois at Urbana-Champaign
Urbana, IL 61801

ABSTRACT

Convective and dispersive transport of a tagged species in a porous medium is investigated analytically. The flow is transient and compressible. As a means of avoiding anomolous numerical dispersion in transport calculations, an Eulerian-Lagrangian technique is developed. The Lagrangian mesh travels along characteristic curves of the convective transport equation. Transport relative to this mesh is dispersive. Detailed calculations are made for low Peclet number transport in the unsteady, low Reynolds number, isothermal flow of an ideal gas through the bed. Results are obtained for a bed of finite length. Similarity, valid for an infinite bed length, yields widely applicable results. The analysis and results are useful in the containment of underground nuclear explosions.

*This work was performed under the auspices of the USERDA and was supported by the University of California Lawrence Livermore Laboratory under Subcontract 1160305 of Contract W-7405-Eng-48.

INTRODUCTION

Following an underground nuclear explosion, gas from the cavity may enter the stemming column or surrounding porous medium. Driven by the high pressure within the cavity, the fluid flows through the porous material. The duration period of this high cavity pressure is typically several minutes. The extent of penetration of cavity gas into the porous material is of interest in containment evaluation.

Single phase [1] and multiphase [2] flow analyses have been presented describing such transient flows. If the absence of gaseous phase dispersion is posited, the gas originally in the medium is displaced in a piston-like manner. A distinct interface then exists between the gas originally in the bed and gas originating in the cavity. The extent of cavity gas penetration is unambiguous and can be determined in a straight forward manner.

In any real flow, however, there is a dispersive transport as well as convective transport. A sharp interface does not exist. Instead, a gradual transition occurs. The purpose, then, of this paper is to analyze and describe the concentration distributions resulting from such transient flows with dispersion. Because the leading cavity fluid is a gas, only an ideal gas flow is considered in detail. We do not examine the multiphase flow following the leading cavity gas.

THE TRANSPORT EQUATION

We consider the transport of an inert trace species, characterized by a concentration c. The species is transported by convection and dispersion. Convective transport results from the directed motion of the carrier fluid. Without dispersion, there is no mixing. Changes in the species concentration within any fluid element would then result solely from compression or expansion of that element. The convective flux across a unit area normal to the direction of flow is

$$j_C = uc \tag{1}$$

u is termed the apparent velocity and is the volume flow rate per unit area.

The dispersion associated with miscible flow within porous media has received a great deal of attention. It is normally assumed that the dispersive flux can be described by Fick's law and can be simply added to the convective flux. For the one-dimensional flow considered here, the dispersive flux is

$$j_D = -\mathcal{D} \frac{\partial c}{\partial x} \tag{2}$$

$\mathcal{D}$ is the dispersion coefficient and x is a position coordinate in the direction of flow. In a two-dimensional flow, the dispersion coefficient for dispersion transverse to the direction of bulk fluid motion is, in general, different from the longitudinal dispersion coefficient. Only longitudinal dispersion is considered here.

The magnitude of the dispersion coefficient depends on the Peclet number, based on grain size, of the fluid flow. For low Peclet number flows, dispersion results primarily from molecular diffusivity. In this range, the dispersion coefficient is essentially independent of Peclet number and is of the order of the molecular diffusion coefficient. In faster flows, additional mixing occurs as a result of the inhomogeneity of the medium. Velocity

variations, path tortuosity, and dead spaces all contribute to increased dispersion. The dispersion coefficient is a monotonically increasing function of the Peclet number, being roughly proportional to Peclet number over a broad range. While theoretical models for the dispersion coefficient are available, dimensionless correlations of experimental results appear to have greater present utility. Reviews [3-4] of analysis and experiment directed toward providing hydrodynamic dispersion coefficients for porous media describe much of the work in this area.

The flows of particular interest here are characterized by Reynolds numbers less than one. Since gas Schmidt numbers are normally of order unity, the corresponding Peclet numbers are small. The dispersion coefficients are taken to be independent of the local velocity and to be of the order of magnitude of the molecular diffusion coefficient.

The molecular diffusion coefficient is itself a function of the thermodynamic state of the gas. The molecular diffusivity in gases increases with increasing temperature and varies inversely with the pressure [5]. Despite the high temperature within a nuclear cavity, the gas flow is isothermal at ambient temperature ahead of the saturation front produced by condensation [2]. While the gas and the solid material will rapidly come to local thermodynamic equilibrium, the heat capacity of the solid greatly exceeds that of the invading gas. Accordingly, the temperature rise from ambient in this portion of the porous medium will be small. Since the pressure will vary by at least an order of magnitude in the same region, the molecular diffusion coefficient, and thus the dispersion coefficient, is taken to vary only with pressure

$$\mathcal{D} = \mathcal{D}_o \frac{p_o}{p} \tag{3}$$

p is the pressure. The subscript o denotes atmospheric conditions.

Conservation of species for an infinitesimal region of space becomes

$$\varepsilon \frac{\partial c}{\partial t} + \frac{\partial}{\partial x} (j_C + j_D) = 0 \tag{4}$$

for a flow in one dimension. ε is the porosity of the medium. t is the time. Using the flux expressions, we have

$$\varepsilon \frac{\partial c}{\partial t} + \frac{\partial}{\partial x} (uc) = \frac{\partial}{\partial x} \left(\mathcal{D} \frac{\partial c}{\partial x} \right) \tag{5}$$

the convective-dispersive transport equation in an Eulerian frame.

THE FLUID MOTION

In order to determine the concentration distribution, the fluid velocity and pressure distributions must first be determined. The forms in which these distributions become known will also affect the subsequent choice of tools utilizing them.

The fluid velocity in a low Reynolds number single phase flow is related to fluid and material properties by Darcy's law. The apparent velocity is

$$u = -\frac{k}{\mu}\frac{\partial p}{\partial x} \tag{6}$$

k is the permeability of the medium. μ is the fluid viscosity. Continuity for a compressible fluid is

$$\varepsilon\frac{\partial \rho}{\partial t} + \frac{\partial}{\partial x}(\rho u) = 0 \tag{7}$$

ρ is the fluid density.

In an isothermal ideal gas, the viscosity may be taken as constant and the local density is directly proportional to the pressure. Combining (6) and (7), we obtain

$$\frac{\partial}{\partial x}\left(p\frac{\partial p}{\partial x}\right) = \frac{\varepsilon\mu}{k}\frac{\partial p}{\partial t} \tag{8}$$

governing the pressure. Permeability is presumed uniform.

Prior to a nuclear explosion, the gas in the medium is at a uniform ambient pressure, p_o. As a boundary condition, we will consider a step change to a higher pressure, p_1, at the inlet. The position, x, is taken as the distance from this inlet. Both semi-infinite and finite media are of interest. The results of analysis of flow in a semi-infinite medium may be applied to flow in a finite porous medium until such time as effects of the flow appear at the distant boundary. The column length is denoted by L.

For numerical calculation, it is convenient to introduce a set of dimensionless variables and to express the governing relations and results in terms of them. Dimensionless position is

$$X \equiv \frac{x}{L} \tag{9}$$

ranging, in the finite bed, from zero at the inlet to one at the distant boundary. Dimensionless time is defined

$$\tau \equiv \frac{k(p_1 - p_o)\, t}{\varepsilon\mu L^2} \tag{10}$$

The ratio of applied to initial pressure is

$$N \equiv \frac{p_1}{p_o} \tag{11}$$

A dimensionless pressure,

$$P \equiv \frac{p - p_o}{p_1 - p_o} \tag{12}$$

also varying between 0 and 1, depends only on X, τ, and N. The governing equation, (8), becomes

$$\frac{1}{2}\frac{\partial^2}{\partial X^2}\left(P^2 + \frac{2P}{N-1}\right) = \frac{\partial P}{\partial \tau} \tag{13}$$

describing flow in a finite bed.

In an unbounded bed, the bed length is infinite and the separate definitions (9) and (10) are not suitable. The length is conveniently removed by the observation that the pressure distribution resulting from a step pressure change at the surface of a semi-infinite porous medium may be expressed in terms of a single variable, θ, rather than position and time separately. Introducing

$$\theta \equiv \frac{X}{2\sqrt{\tau}} = \frac{x}{2}\sqrt{\frac{\varepsilon\mu}{k(p_1 - p_o)\, t}} \tag{14}$$

we find that the governing partial differential equation (13) becomes the ordinary differential equation

$$\frac{d^2}{d\theta^2}\left(P^2 + \frac{2P}{N-1}\right) + 4\theta\frac{dP}{d\theta} = 0 \tag{15}$$

subject to the boundary conditions

$$\begin{aligned} P &= 1 \quad \text{at} \quad \theta = 0 \\ P &\to 0 \quad \text{as} \quad \theta \to \infty \end{aligned} \tag{16}$$

The flow is similar. Note that the characteristic length L does not appear in θ.

Flows governed by (13), or alternatively, (15) were analyzed in [1] and results presented. In the results to be presented here, all fluid flow calculations are numerical solutions of (13). For short times, until changes occur at the distant boundary, the flow in a finite column is identical to that in the infinite column. Pressures found as a function of position and time, can be expressed as a function of the similarity variable by using (14). The early time flow is similar. Attention was devoted to the analysis of finite columns because the results are more general and because semi-infinite bed results are readily extracted from short time finite column calculations. Furthermore, a reduction in the number of variables, producing an ordinary differential equation, does not necessarily simplify the numerical solution. It may be noted, in this context, that boundary conditions (16) include a condition at infinite θ.

Equation (13) is analogous to a nonlinear heat conduction equation. The numerical procedure selected for its solution is the method of Bruce, Peaceman, Rachford, and Rice [6]. The procedure is implicit and unconditionally stable. It is similar to the Crank-Nicolson [7] method for solution of the linear diffusion equation. Because (13) is nonlinear, the Bruce, Peaceman, Rachford, and Rice procedure is iterative. Its convergence is rapid. Moreover, the

coefficient matrix of the finite difference equations is tridiagonal so that each iteration is efficiently performed. An algorithm [8] for the solution of a tridiagonal set of n equations requires only 5n - 2 storage locations and a number of operations of order n.

TRANSPORT IN LOW REYNOLDS NUMBER FLOW

Before proceeding, the convection-dispersion equation may also be put into dimensionless form. Suitable parameters were introduced in the discussion of fluid motion. A dimensionless speed,

$$U \equiv \frac{\mu L u}{k(p_1 - p_o)} \tag{17}$$

would be unity in an incompressible Darcy flow. A reduced concentration is expressed in terms of the concentration of entering gas, c_1.

$$C \equiv \frac{c}{c_1} \tag{18}$$

The dimensionless dispersivity is defined by

$$D \equiv \frac{\mu \mathcal{D}}{k(p_1 - p_o)} \tag{19}$$

and expresses the relative importance of dispersive and convective transport. It is roughly the inverse of a Peclet number based on bed length. In terms of these additional variables, equation (5) becomes

$$\frac{\partial c}{\partial \tau} + \frac{\partial}{\partial X}(UC) = \frac{\partial}{\partial X}\left(D \frac{\partial C}{\partial X}\right) \tag{20}$$

The dimensionless speed, U, is the speed of a fluid element in the dimensionless coordinates. In dimensional coordinates, this speed is the "pore velocity"

$$\frac{u}{\epsilon} = \frac{-k}{\mu \epsilon} \frac{\partial p}{\partial x} \tag{21}$$

Changing variables yields

$$U = - \frac{\partial P}{\partial X} \tag{22}$$

Introducing this expression for U in terms of the dimensionless pressure gradient into transport equation (20), we note that this partial differential equation may be written as an ordinary differential equation in the same

similarity variable as describes the pressure.

$$\frac{d}{d\theta}\left(C\frac{dP}{d\theta}\right) + 2\theta\frac{dC}{d\theta} + \frac{d}{d\theta}\left(D\frac{dC}{d\theta}\right) = 0 \tag{23}$$

Since the initial concentration throughout the medium is zero and since the inlet concentration is given a step change to a constant value, the initial and boundary conditions are compatible with a similarity solution.

$$\begin{aligned} C &= 1 \quad \text{at} \quad \theta = 0 \\ C &\to 0 \quad \text{as} \quad \theta \to \infty \end{aligned} \tag{24}$$

The concentration distribution in the semi-infinite medium is similar and is expressed in terms of the same variable, θ, as is the pressure. Although strictly valid only for semi-infinite medium, the similarity may be used with great accuracy in a finite bed until such time as effects of the flow appear at the distant boundary.

A finite column requires an examination of conditions to be imposed at the distant boundary. For an open column, the exit pressure is taken to be equal to the initial pressure. The solution of (14) requires such a boundary condition as well as the initial condition and inlet boundary condition previously imposed. In the absence of dispersion, no exit boundary condition is required for the solution of (20). With dispersion, however, a boundary condition becomes necessary. The form of this exit boundary condition on concentration is not obvious. Convective and dispersive fluxes within the porous bed and directed toward this surface must be coupled to fluxes leading from this surface and outside the bed. Test conditions beyond the medium are subject to considerable variation. Moreover, containment efforts seek to predict, and then prevent, any measurable concentration of cavity gas at the surface. Accordingly, we simply take as this boundary condition the widely used Danckwerts [9] condition for the exit of a chemical reactor. The dispersive flux, given by (2), is set equal to zero at the exit.

This condition has been extensively employed in both steady state and unsteady state analyses. As noted by Wehner and Wilhelm [10] however, its use in the unsteady state is strictly valid only when the Peclet number is infinite in the region beyond the bed.

NUMERICAL DISPERSION

Because an Eulerian approach is used to determine the velocity, pressure, and dispersivity distributions, Eulerian methods should be considered for subsequent analysis of trace component transport. Eulerian techniques, however, tend to produce an anomolous numerical dispersion which can exceed the physical dispersion of interest here. Noh and Protter [11] analyzed the diffusion resulting from a finite difference approximation to the linear convection equation.

Consider briefly, as an example, the linear convective transport in an incompressible flow. In this simple case, equation (20) reduces to

$$\frac{\partial C}{\partial \tau} + U \frac{\partial C}{\partial X} = 0 \tag{25}$$

with a constant velocity, U, and having

$$X = X_o + U\tau \tag{26}$$

as a characteristic curve. The concentration, C, is constant on a characteristic. There is no physical dispersion.

Further, consider a finite difference approximation to (25) which is forward in time and employs upwind differencing.

$$\frac{C_i^{k+1} - C_i^k}{\Delta\tau} + U \frac{C_i^k - C_{i-1}^k}{\Delta X} = 0 \tag{27}$$

The index denoting the time level is the superscript k. The subscripts, i, are spacial indices in the uniform Eulerian mesh. Using Taylor series expansions for the concentration, neglecting terms above second order, and using (25), we find that (27) is equivalent to

$$\frac{\partial C}{\partial \tau} + U \frac{\partial C}{\partial X} = \frac{U\Delta X}{2}\left(1 - \frac{U\Delta\tau}{\Delta X}\right)\frac{\partial^2 C}{\partial X^2} + \ldots \tag{28}$$

The coefficient of the second spatial derivative on the right-hand side is a numerical dispersion coefficient. It has no physical basis but arises

from the use of the finite difference expressions. Numerical dispersion coefficients of this type can exceed the actual dispersion coefficient by orders of magnitude. For small Courant number, $U\Delta T/\Delta X$, the ratio of these terms is roughly $U\Delta X/D_o$ which we shall call the "cell Peclet number." D_o is the dimensionless dispersivity at ambient conditions.

Because the flow actually being investigated is transient and compressible and possesses physical dispersion, the situation is considerably more complex. The velocity varies with position and time. Techniques developed to reduce artificial dispersion in Eulerian calculations, but relying on a uniform fluid velocity, e.g. [12], are not applicable. Accordingly, a mixed Eulerian-Lagrangian approach was considered, developed, and then adopted. In addition to the fixed uniform Eulerian grid used to calculate pressure, velocity, and the dispersion coefficient, a moving nonuniform Lagrangian mesh is used to determine the concentration, c, of the transported trace component. The method yields accurate results independent of cell Peclet number.

LAGRANGIAN FORMULATION

A Lagrangian observer moves, with a fluid element, along a characteristic curve of the convective transport equation. The velocity of a Lagrangian mesh point is, in dimensionless coordinates,

$$\frac{dX}{d\tau} = U \tag{29}$$

There is no convective transport between Lagrangian cells. Such transport occurs solely as a result of dispersion. The numerical dispersion of the Eulerian approach resulted from convective transport through the Eulerian mesh. When a Lagrangian viewpoint is adopted, there is no such transport and no numerical mechanism producing such transport is generated. The Lagrangian approach provides a natural means of eliminating artificial dispersion, valid for compressible flow and for flow with physical dispersion. A Lagrangian technique has been used by Garder, Peaceman, and Pozzi [13] to treat dispersion in an incompressible flow through porous media. Their analysis did not address the myriad effects of compressibility. The technique described here differs in that respect, includes variable dispersivity, and differs in the means of calculating dispersive transport.

A temporal derivative in the Lagrangian frame is expressed by the material or substantial derivative

$$\frac{d}{d\tau} = \frac{\partial}{\partial\tau} + U\frac{\partial}{\partial X} \tag{30}$$

so that the convective-dispersive transport equation, (20) becomes

$$\frac{dC}{d\tau} + C\frac{\partial U}{\partial X} = \frac{\partial}{\partial X}\left(D\frac{\partial C}{\partial X}\right) \tag{31}$$

The first term on the left-hand side of (31) is the rate of change of concentration in a fluid element. This concentration change results from dispersive transport into the fluid element, expressed on the right-hand side,

and also, when the flow is compressible, from the compression or expansion of the fluid element. This last contribution is expressed in the second term on the left-hand side of (31).

As a consequence of this compressibility, the concentration is not constant on a characteristic curve even in the absence of dispersion. Additionally, the spacing between successive Lagrangian mesh points will vary as they travel through the medium. Neither of these effects are present in an incompressible flow.

CONVECTIVE TRANSPORT

First, let us address the problem of calculating the positions of the points in the nonuniform expanding Lagrangian mesh. The instantaneous velocity of any Lagrangian mesh point, ℓ, is given by (29). In a low Reynolds number flow, this velocity is given in terms of the pressure gradient by equation (22). The problem then reduces to one of interpolating to obtain the pressure gradient at the location of ℓ. The pressure is known, from fluid flow calculations, at each of the Eulerian nodes. These Eulerian nodes are separated by intervals of ΔX and the Lagrangian node, ℓ, is located at some distance, $f\Delta X$, in front of the nearest Eulerian node, i.

$$|f| \leq \frac{1}{2} \tag{32}$$

Using the pressures at three Eulerian nodes, i-1, i, and i+1, the pressure gradient, and thus the velocity, at the Lagrangian node is found with error of order ΔX^2.

$$\left.\frac{\partial P}{\partial X}\right|_{\ell} = \frac{(2f + 1)\, P_{i+1} - 4f\, P_i + (2f - 1)\, P_{i-1}}{2\Delta X} - \frac{1 - 3f^2}{6} \Delta X^2 \left.\frac{\partial^3 P}{\partial X^3}\right|_{\ell} + \ldots \tag{33}$$

Numerical integration of velocity yields the Lagrangian node position as a function of time. Because the local fluid velocity varies with position and time, however, the node velocity during a time interval ΔT is better approximated by a mean of calculated velocities at the two time levels and at the old and new positions. Since the new position is unknown until the calculation is complete, an iterative procedure to determine the new position is employed. A single iteration appears to be adequate in our application. A criterion used to judge the adequacy of the convective transport calculations is described in a later section on application and results. Time centering of Lagrangian node motion calculations has previously been proposed by Forester [14].

We may now consider the concentration changes resulting from the expansion or compression of a fluid element. This contribution to the variation of concentration is described by the convective transport equation, (31) with dispersivity set to zero.

$$\frac{dC}{d\tau} + C\,\frac{\partial U}{\partial X} = 0 \tag{34}$$

The velocity gradient, $\partial U/\partial X$, is positive in an expanding flow and negative in a compressing flow. It can be calculated by a variety of methods. The method recommended here, however, is to eliminate the calculation entirely with the following conservation.

The bulk fluid density obeys a convective transport equation identical to (34). The continuity equation, (7), in a Lagrangian frame and written in dimensionless coordinates is

$$\frac{dp}{d\tau} + \rho\,\frac{\partial U}{\partial X} = 0 \tag{35}$$

The concentration of a fluid element changes in proportion to the density. Because the density in an isothermal ideal gas is proportional to the fluid pressure, the concentration becomes proportional to the pressure of the fluid element. In dimensionless form, this becomes

$$C \sim (N - 1)\,P + 1 \tag{36}$$

The pressure at Lagrangian node, ℓ, is found by interpolating between the Eulerian nodes where the pressure is known.

$$P_\ell = \frac{f(f+1)}{2}\,P_{i+1} + (1 - f^2)\,P_i + \frac{f(f-1)}{2}\,P_{i-1} - \frac{1}{6}\,f(1 - f^2)\,\Delta X^3\,\left.\frac{\partial^3 P}{\partial x^3}\right|_\ell + \ldots \tag{37}$$

The error is of order ΔX^3. Equation (33) for the pressure gradient is simply a derivative of (37).

In the general case of convective-dispersive transport, the concentration, because of dispersivity, does not remain proportional to the pressure. Instead, the concentration change for a single time step is separated into convective and dispersive changes. Starting with the concentration, C_ℓ^k, of the ℓth Lagrangian node at time level k, the convective contribution yields an intermediate value of the new concentration at the succeeding time level.

$$C_\ell^{k+1} = C_\ell^k \frac{(N-1)\, P_\ell^{k+1} + 1}{(N-1)\, P_\ell^k + 1} \tag{38}$$

This intermediate spatial distribution of concentration is then used to determine how dispersion alters the concentration distribution at this time level. Note that, without explicitly introducing dispersion, no dispersion is generated. In the Lagrangian calculation of convective transport, a moving node with zero concentration at any time has zero concentration for all time.

DISPERSIVE TRANSPORT

Dispersive transport is governed by the diffusion equation, equation (20), with the fluid velocity set equal to zero.

$$\frac{dC}{d\tau} = \frac{\partial}{\partial X}\left(D\,\frac{\partial C}{\partial X}\right) \tag{39}$$

Its solution here is complicated only by the fact that the Lagrangian mesh is nonuniform.

In order to find the concentration at time level k + 1, the Lagrangian grid is held in its k + 1 configuration. The intermediate concentrations, calculated to account for expansion and described in the previous section, are treated as the concentrations at time level k but in the new positions. The order of operations is as if the node movement and fluid expansion occur instantaneously, then the tagged species disperses through the stationary fluid during the time interval $\Delta\tau$.

The finite difference approximation to the diffusion equation (18) is developed in an analogous form to techniques widely used in the solution for a uniform mesh. For a uniform mesh, one could write

$$C_\ell^{k+1} - C_\ell^k = \frac{\Delta\tau}{\Delta X^2}\left\{\beta[\delta(D\delta C)]^{k+1} + (1-\beta)\,[\delta(D\delta C)]^k\right\} \tag{40}$$

δ is the central difference operator. β is a factor weighting the calculation of the second spatial derivative between levels k and k + 1.

β is zero for an explicit calculation. For constant dispersivity, the behavior of (40) is well known. When β is 1/2, this is the Crank-Nicolson method having truncation error of order $\Delta\tau^2$, ΔX^2. More generally, the error is of order $\Delta\tau$, ΔX^2. For $\beta \geq 1/2$, the calculation is unconditionally stable. Note that the coefficient matrix of the unknown concentrations is tridiagonal so that the same efficient algorithm as was used to calculate pressure could be used here.

When treating the nonuniform mesh, it is desirable to retain a tridiagonal form because of the considerable savings in computational time. There is a penalty in accuracy, however. A three-point approximation to the second derivative, for example, has a lower order error than the uniform mesh equivalent.

$$\left.\frac{\partial^2 C}{\partial x^2}\right|_{\ell} = \frac{2C_{\ell+1}}{(X_{\ell+1} - X_{\ell})(X_{\ell+1} - X_{\ell-1})} - \frac{2C_{\ell}}{(X_{\ell+1} - X_{\ell})(X_{\ell} - X_{\ell-1})}$$

$$+ \frac{2C_{\ell-1}}{(X_{\ell} - X_{\ell-1})(X_{\ell+1} - X_{\ell-1})} - \frac{1}{3}(X_{\ell+1} - 2X_{\ell} + X_{\ell-1}) \left.\frac{\partial^3 C}{\partial x^3}\right|_{\ell} + \ldots \tag{41}$$

The leading error term vanishes for a uniform mesh. A nonuniform mesh should be generated so as to maintain small values for these additional error terms. A smooth slow variation of mesh size is best from this standpoint.

With varying diffusivity, the nonuniform mesh equivalent of (40) was taken as

$$\frac{C_{\ell}^{k+1} - C_{\ell}^{k}}{\Delta\tau} = \frac{2\beta}{X_{\ell+1} - X_{\ell-1}} \left(D_{\ell+(1/2)} \frac{C_{\ell+1} - C_{\ell}}{X_{\ell+1} - X_{\ell}} - D_{\ell-(1/2)} \frac{C_{\ell} - C_{\ell-1}}{X_{\ell} - X_{\ell-1}} \right)^{k+1}$$

$$+ \frac{2(1-\beta)}{X_{\ell+1} - X_{\ell-1}} \left(D_{\ell+(1/2)} \frac{C_{\ell+1} - C_{\ell}}{X_{\ell+1} - X_{\ell}} - D_{\ell-(1/2)} \frac{C_{\ell} - C_{\ell-1}}{X_{\ell} - X_{\ell-1}} \right)^{k} \tag{42}$$

$D_{\ell+(1/2)}$ is the dimensionless dispersivity midway between Lagrangian nodes ℓ and $\ell + 1$.

For β equal to 1/2, a slight oscillation was observed in the results. Since the variable diffusivity and nonuniform mesh preclude the possibility of a higher order error associated with β equal to 1/2, there need be no

reluctance to vary β. For stability, a weighting factor, β, greater than 1/2 is recommended. No oscillation has been observed for larger β.

APPLICATION AND RESULTS

A program, DIASPORA, employing these methods has been written and applied to the transient convective-dispersive transport in a porous medium. Consider, as an example, the transport resulting from a step increase in pressure and concentration at one end of a uniform porous bed. The bed is finite with the other end open to the atmosphere. The initial concentration in the bed is zero. The resulting pressure and concentration distributions are of interest in containment calculations. Pressure distributions have previously been obtained for ideal gas [1] and multiphase [2] flows of this type. We here obtain the concentration distribution associated with the ideal gas flow.

Following [1] and [2], consider a flow characterized by a pressure ratio, N, of 45. This value is obtained from Olsen's [15] description of the cavity pressure history of an underground nuclear explosion in alluvium. The pressure distribution in the bed, governed by (13), was found and is shown in Fig. 1. As the pressure increase propagates through the medium, the region of higher pressure is clearly discernible. A near discontinuity is present in the pressure gradient as a pressure front seems to travel through the bed. For higher pressure ratio, N, the initial pressure rise at any location is even sharper. When the pressure ratio is infinite, this pressure rise is discontinuous. Because of this behavior, the far boundary has little effect on the flow for a well defined period. For an infinite pressure ratio, the pressure front reaches the exit when τ is 0.38. Prior to this time, the flow is similar and the pressure depends on the single variable, θ, defined by (13). For large but finite pressure ratio, N, the similarity is not rigorously exact but is an excellent approximation until τ is about 0.38. This similarity can be seen

in Fig. 1 where positions on the $\tau = 0.2$ curve are twice the corresponding positions on the $\tau = 0.05$ curve. The pressure calculation is Eulerian, using the procedure of Bruce, Peaceman, Rachford, and Rice [6].

The corresponding concentration distribution in the absence of dispersion is presented in Fig. 2. The Lagrangian formulation yields the abrupt change in concentration as the injected gas passes through the column. This feature would not be observed if an Eulerian expression such as (27) were employed. Note also that the early time behavior is very nearly similar. The effects of the distant boundary are not apparent for τ less than about 0.38. As with the pressure, θ is the sole independent variable in a similar flow. The positions of corresponding points on the short time curves vary as the square root of time. The agreement among the calculated concentration distributions in this regard is an excellent indication of the accuracy of the calculations.

The position of the interface is a particularly stringent and readily observed indication of this accuracy. When τ is 0.05, the position of the interface was calculated to be 0.30. Accordingly, the calculated value of θ at the interface is, from (14), 0.67. Since the flow is nearly similar for time less than 0.38, θ at the interface should remain relatively constant prior to this time. For times of 0.1, 0.2, and 0.3, the calculated positions correspond to θ being 0.67, 0.68, and 0.68, respectively. The initial step change in pressure at the interface is responsible for making this Lagrangian node the most difficult to move accurately.

The concentration curves for times 0.5 and 3.0 are shown ending before the exit. The reason is simply that the plotting routine used to generate the curves used the Lagrangian node nearest the exit as the final point. All leading nodes have exited in both cases. Because the concentration

remains proportional to pressure in convective transport, the exit concentration C is N^{-1} or 45^{-1} for both curves.

Figures 3 through 5 show the effect of dispersivity. Variable dispersivity is employed in each case. At ambient pressure, the dimensionless dispersivity is 10^{-3}, 10^{-2}, and 10^{-1}, respectively, in these figures. The dimensionless dispersivity at ambient conditions D_o can be estimated in any application using (19). Using air viscosity of 1.8×10^{-5} kg/m sec, a diffusivity of 2×10^{-5} m^2/sec, a permeability of 0.1 darcy (9.8×10^{-14} m^2) and the applied pressure difference of 44×10^5 pa, the dimensionless dispersivity D_o is of order 10^{-3}. The dimensionless dispersivity would be larger in less permeable media, smaller in more permeable media. The permeability determines the rate of convective transport. With convective-dispersive transport, application of the Danckwerts boundary condition, zero concentration gradient, at the exit yields the concentration there.

Each of the calculations presented used an Eulerian grid having 101 nodes. The time step was $2 \times 10^{-4}/3$ for 225 steps, then changed to 10^{-3}. The smaller initial time step is used to prevent large initial Lagrangian node movement. With either time step and presuming U to be of order unity, the numerical dispersion expressed by (28) is of order 10^{-2}. This numerical dispersion would be large compared to physical dispersion. The cell Peclet number is about 10 for the example just given. The simple Eulerian approach would not have yielded useful results.

CONCLUSIONS

Convective and dispersive transport in transient compressible flow has been analyzed. The governing relations were formulated and a numerical procedure for calculating results was presented. Reasons for utilizing an Eulerian-Lagrangian approach were considered. Techniques for accurately determining mesh movement, fluid expansion, and trace element dispersion are described. Results were presented for transport resulting from a transient flow of an isothermal ideal gas through a uniform porous bed.

FIGURE LEGENDS

Figure 1 Pressure distribution in unsteady flow

Figure 2 Concentration distribution in convective transport

Figure 3 Concentration distribution in convective-dispersive transport with varying dispersivity

Figure 4 Concentration distribution in convective-dispersive transport with varying dispersivity

Figure 5 Concentration distribution in convective-dispersive transport with varying dispersivity

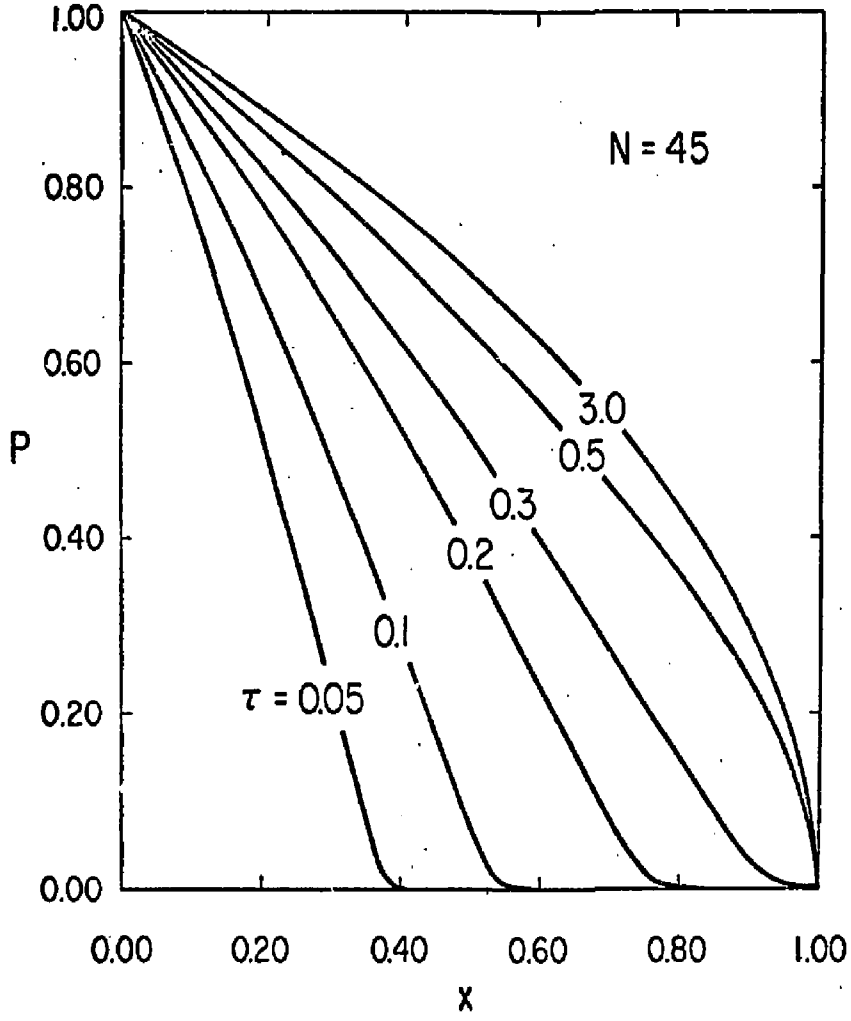

Figure 1 Pressure distribution in unsteady flow

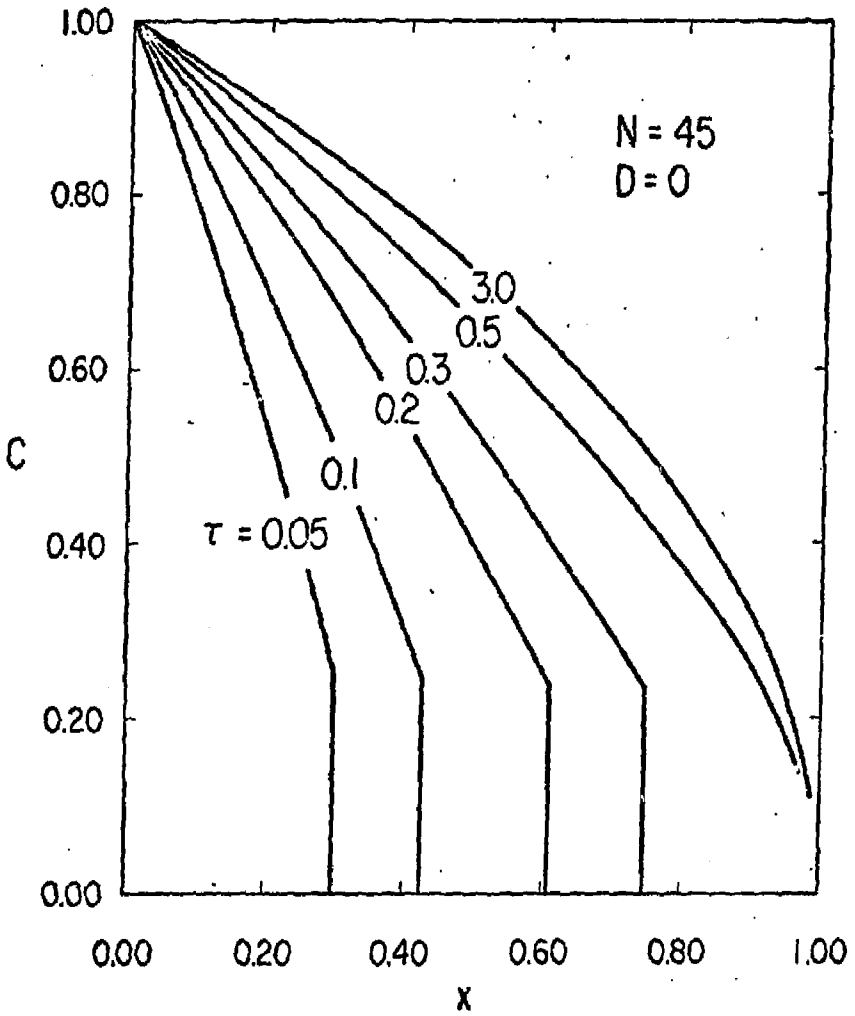

Figure 2 Concentration distribution in convective transport

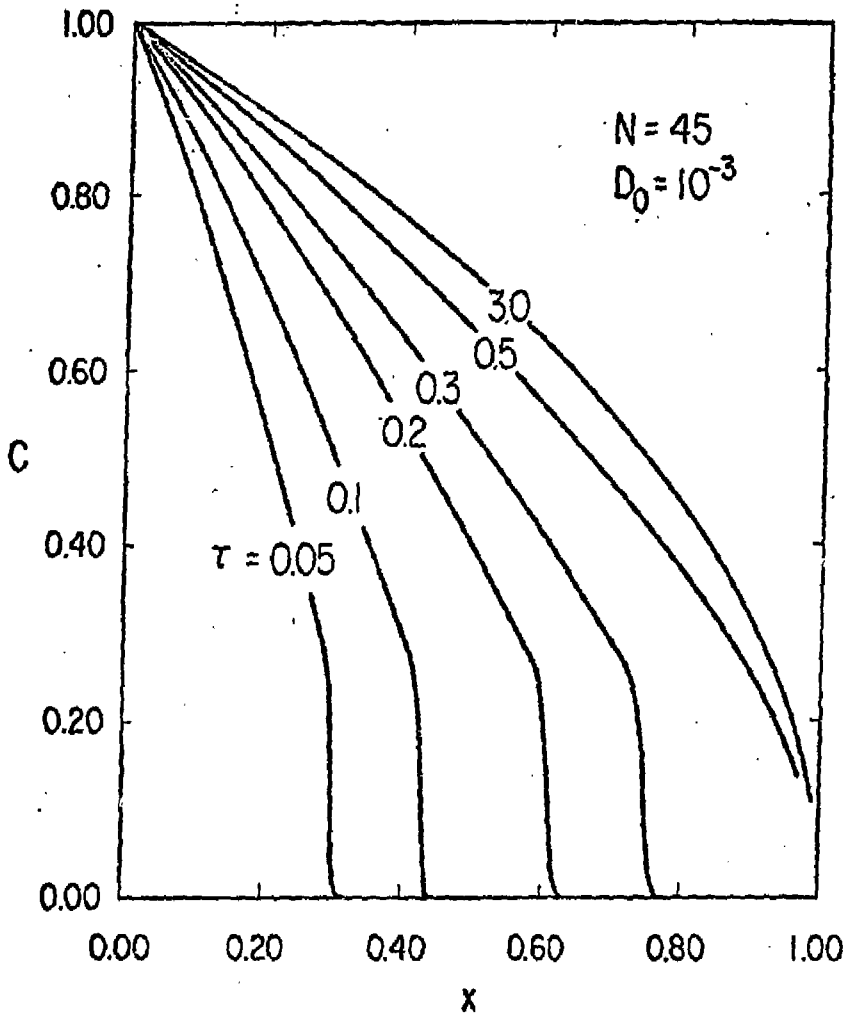

Figure 3 Concentration distribution in convective-dispersive transport with varying dispersivity

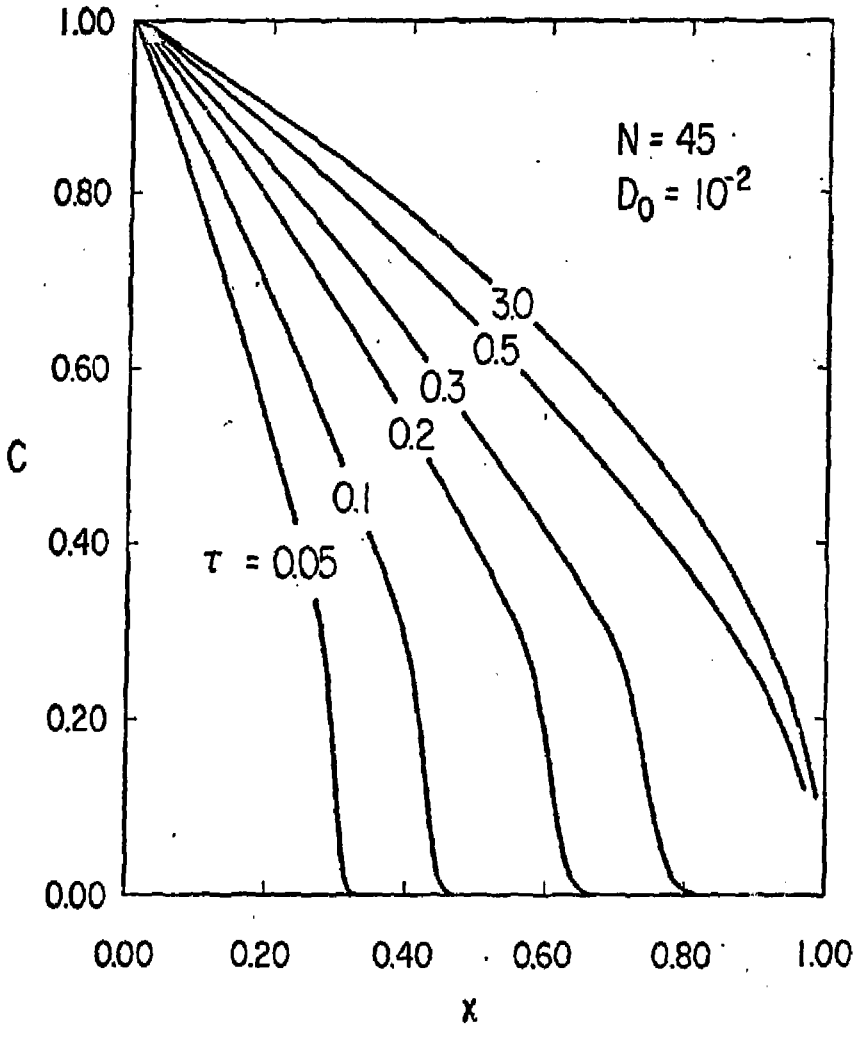

Figure 4 Concentration distribution in Convective-dispersive transport with varying dispersivity

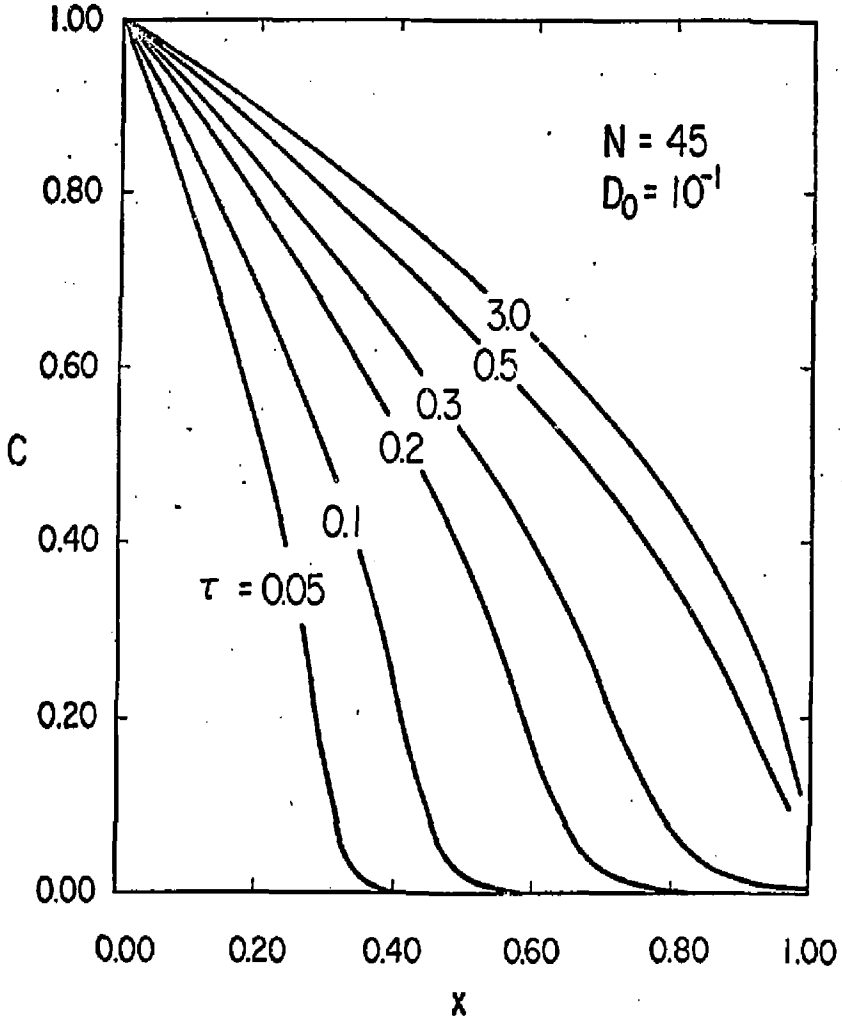

Figure 5 Concentration distribution in convective-dispersive transport with varying dispersivity

REFERENCES

1. F. A. Morrison, Jr., Transient gas flow in a porous column, Ind. Eng. Chem. Fundam. 11, 191 (1972).
2. F. A. Morrison, Jr., Transient multiphase multicomponent flow in porous media, Int. J. Heat Mass Transfer, 16, 2331 (1973).
3. T. K. Perkins and O. C. Johnston, A review of diffusion and dispersion in porous media, Trans. Am. Inst. Min. Engrs. 228, 70 (1963).
4. J. Bear, Dynamics of Fluids in Porous Media, American Elsevier, New York (1972).
5. J. O. Hirschfelder, C. F. Curtiss, and R. B. Bird, Molecular Theory of Gases and Liquids, Wiley, New York (1954).
6. G. H. Bruce, D. W. Peaceman, H. H. Rachford, Jr., and J. D. Rice, Calculations of unsteady-state gas flow through porous media, Trans. Am. Inst. Min. Engrs. 198, 79 (1953).
7. J. Crank and P. Nicolson, A practical method for numerical evaluation of solutions of partial differential equations of the heat conduction type, Proc. Camb. Phil. Soc. 43, 50 (1947).
8. R. W. Hornbeck, Numerical marching techniques for fluid flows with heat transfer, NASA SP-297 (1973).
9. P. V. Danckwerts, Continuous flow systems, Chem. Eng. Sci. 2, 1 (1953).
10. J. F. Wehner and R. H. Wilhelm, Boundary conditions of flow reactor, Chem. Eng. Sci. 6, 89 (1956).
11. W. F. Noh and M. H. Protter, Difference methods and the equations of hydrodynamics, J. Math. and Mech. 12, 149 (1963).
12. H. L. Stone and P. L. T. Brian, Numerical solution of convective transport problems, Am. Inst. Chem. Eng. J. 9, 681 (1963).

13. A. O. Garder, Jr., D. W. Peaceman, and A. L. Pozzi, Jr., Numerical calculation of multidimensional miscible displacement by the method of characteristics, Trans. Am. Inst. Min. Engrs. 231, 26 (1964).

14. C. K. Forester, A method of time-centering the Lagrangian marker particle computation, J. Comp. Phys. 12, 269 (1973).

15. C. W. Olsen, Time history of the cavity pressure and temperature following a nuclear detonation in alluvium, J. Geophys. Res. 72, 5037 (1967).

APPENDIX C

TRANSIENT NON-DARCY GAS FLOW IN A POROUS MEDIUM

F. A. Morrison, Jr.

TRANSIENT NON-DARCY GAS FLOW IN A POROUS MEDIUM*

F. A. Morrison, Jr.
Member, SPE
University of Illinois at Urbana-Champaign
Urbana, IL 61801

ABSTRACT

The high Reynolds number flow of gas through porous materials is a subject of increasing significance. Gas recovery from fractured beds, gas flow produced by *in situ* coal gasification, flows associated with storage and withdrawal in highly permeable structures, and transpiration cooling are examples. Darcy's law, normally used to describe flows through porous materials, is invalid in the range of Reynolds number of interest here. A nonlinear constitutive equation with empirically determined transport properties is applicable instead.

Transient, compressible gas flow over a broad range of Reynolds number has been analyzed. The flow is governed by a set of coupled nonlinear partial differential equations. An iterative implicit stable numerical procedure has been developed and successfully tested for calculations in one dimension. Results are given for the flow resulting from a step change in pressure at one end of a finite bed. A similarity solution is obtained for the flow into a semi-infinite bed. This latter solution is also applicable to short time flow in finite beds.

*This work was performed under the auspices of the USERDA and was supported by the University of California Lawrence Livermore Laboratory under Subcontract 1160305 of Contract W-7405-Eng-48.

INTRODUCTION

The high speed flow of a gas through a porous structure is a matter of considerable interest in several areas. This interest has resulted in a wealth of experimental information on such flows. In particular, Darcy's law, a linear constitutive equation between the apparent fluid velocity and the local pressure gradient, is found to fail for Reynolds numbers in excess of about 0.1. Correlations, describing the deviations from Darcy's law, have been developed and have remarkable agreement among themselves and with experiment.

The analytical ability to use these results in the prediction of more complex flows has not been obtained, however, While transient gas flows in the Darcy regime have been successfully analyzed and efficient algorithms for the calculation of multidimensional flows developed, little progress has been made in the nonlinear flow regime.

The purposes of this paper are to obtain relations governing non-Darcy, transient compressible flow, to develop a numerical procedure for calculations in one dimension, and to present results of the analysis of such a flow.

DESCRIPTION OF THE FLOW

Consider the one-dimensional flow of a gas through a porous structure. The apparent velocity of a fluid flowing through a porous bed is, by definition, the volume flow rate per unit area normal to the direction of flow. In a low Reynolds number flow, this velocity, u, is given by a linear constitutive equation, Darcy's law.

$$u = - \frac{k}{\mu} \frac{\partial p}{\partial x} \tag{1}$$

k is the permeability of the medium, μ is the fluid viscosity, p is the fluid pressure, and x is the position coordinate in the direction of flow. For local Reynolds number, $\rho ud/\mu$, based on pore or grain size d and above about 0.1, this relation is unsatisfactory. ρ is the fluid density. Because of the highly curved tortuous paths followed by fluid elements, inertial effects become significant. The relation between velocity and pressure gradient becomes nonlinear.

Forchheimer [1]* proposed that Darcy's law be modified by the inclusion of a second order term in velocity. In the usual format, Forchheimer's relation is written.

$$a_1 u + a_2 \rho u^2 = - \frac{\partial p}{\partial x} \tag{2}$$

Since this relation was originally proposed, an impressive amount of experimental evidence has been amassed to justify its use. In the low velocity range, the relation reduces to Darcy's law. The constant, a_1, is simply μ/k and can be determined experimentally or, for uniform beds, the widely used Carman-Kozeny relationship [2] or Happel's [3] free surface model yield

*Numbers in brackets refer to entries in REFERENCES.

good estimates. At high velocities, the Forchheimer relation reduces to the form found experimentally by Burke and Plummer [4]. From the Darcy range, spanning a transition region, and up to Reynolds numbers of several thousand, the complete Forchheimer relation has accurately described results of experiments by numerous investigators. These include Ergun and Orning [5], Green and Duwez [6], Ergun [7], Schneebeli [8], and Ward [9]. Theoretical developments of the Forchheimer relation, e.g., Irmay [10], Bachmat [11], and Black [12], having varying degrees of sophistication are also available.

A further generalization of (2) was proposed by Polubarinova-Kochina [13] and consists of the inclusion of a local acceleration term.

$$-a_1 u + a_2 \rho u^2 + a_3 \rho \frac{\partial u}{\partial t} = -\frac{\partial p}{\partial x} \tag{3}$$

t is the time. Because disturbances propagate across a pore having a typical dimension d with a relaxation time of order d^2/ν, this effect is negligible. ν is the kinematic viscosity. For air at atmospheric conditions, ν is 0.15 cm^2/sec. A bed with a permeability of one Darcy (9.8×10^{-9} cm^2) has a typical pore dimension of order 10^{-3}cm. The corresponding relaxation time is of order 10^{-5} sec, considerably less than any significant time in a transient flow. Including this local acceleration effect has no obvious merit.

The effect of convective acceleration, as considered by Beavers and Sparrow [14], is expressed in the relation used by them. In a form consistent with our notation, they have

$$a_1 u + a_2 \rho u^2 + \frac{1}{\varepsilon^2} \rho u \frac{\partial u}{\partial x} = -\frac{\partial p}{\partial x} \tag{4}$$

ε is the porosity of the medium, the void volume fraction. The inertial coefficient, a_2, is of the order of the reciprocal pore dimension, d^{-1}.

The length, d, is considerably smaller than any bed length of interest here. Variations in the apparent velocity occur over distances much larger than d. Accordingly, the quadratic resistance term greatly exceeds the convective acceleration contribution and the latter is safely neglected.

An excellent verification of this conclusion is provided by recent results of Masha, Beavers, and Sparrow [15]. Compressible steady gas flow in one dimension was examined in a series of careful experiments where gas compressibility was significant. The porous medium was a block of foamed nickel with a mean pore size of roughly 0.05 in. and a length of 8 in. The length scale for velocity changes is this bed length. The relative importance of convective acceleration and inertial drag should then be approximately the ratio 0.05:8. The contribution of convective acceleration should, in this case, be roughly 0.6 percent of the effect of inertial drag. Masha, Beavers, and Sparrow found that experimental pressures and calculated pressures based on Eq. (4) agreed within 2 percent. They further found that calculations based on Eq. (2) normally agreed with those employing convective acceleration within 0.1 percent. At the highest test Reynolds number reported, 81.6, the deviation was about 0.7 percent. The two expressions agree within the expected range and both agree well with experiment. For larger beds, with correspondingly smaller pore size-to-bed length ratios, the difference between expressions will be smaller yet.

We conclude that Forchheimer's relation (2) adequately describes the resistance of transient compressible flow over a broad range of Reynolds number. Accordingly, this relation is adopted and, in agreement with Darcy's law, written

$$u + b\,\rho|u|\,u = -\frac{k}{\mu}\frac{\partial p}{\partial x} \tag{5}$$

The quadratic term u^2 is here replaced by $|u|u$ to account for flow in either direction. $|u|$ is the absolute value of u. The coefficient b can be determined from any of several correlations. Typical are those of Ergun [7] and Ward [9] which yield

$$b = \frac{d}{85.7\mu\ (1 - \varepsilon)} \tag{6}$$

and

$$b = \frac{0.550\ (k)^{1/2}}{\mu} \tag{7}$$

respectively.

In addition to the constitutive equation describing flow resistance, the flow obeys the continuity equation, an equation of state and the first law of therodynamics. Conservation of mass is

$$\varepsilon \frac{\partial \rho}{\partial t} + \frac{\partial}{\partial x} (\rho u) = 0 \tag{8}$$

for an incompressible porous structure. The ideal gas equation of state is

$$p = \rho RT \tag{9}$$

R is the gas constant and T, the thermodynamic temperature.

Rather than employing the first law of thermodynamics, it normally suffices to assume an isothermal flow. The relaxation time for heat transfer between the solid and gas is negligible compared with the time for the gas flow to respond to changes at the bed boundaries. Temperature equality between solid and gas is usually assumed. In a gas flow, the heat capacity of the gas in the void volume is considerably less than that of the surrounding solid. As a result, the solid temperature will normally remain constant and the gas temperature rapidly approaches this value. With the isothermal restriction, an ideal gas flow is governed by

Eq. (5) and Eq. (8) which become

$$u + (b/RT)\ p\ |u|\ u = -\frac{k}{\mu}\frac{\partial p}{\partial x} \tag{10}$$

and

$$\epsilon\frac{\partial p}{\partial t} + \frac{\partial}{\partial x}(pu) = 0 \tag{11}$$

Pressure and velocity are the sole independent variables.

Equivalent expressions for radial flow in cylindrical coordinates have been successfully employed [16,17] to describe the performance of natural gas wells. Transient high speed gas flow in one dimension has been examined more recently [18]. In this latter case, however, the second-order differential equation describing the flow is incorrect as given.

DIMENSIONLESS FORM

Because the governing equations, Eqs. (10) and (11), are nonlinear, their solution is most readily obtained using numerical techniques. Prior to developing a numerical procedure, it is advantageous to convert these expressions to a dimensionless form. The dimensionless expressions are chosen to correspond closely with those used in the analysis of related low Reynolds number gas flow [19], low Reynolds number multiphase flow [20] and low Reynolds number convective-dispersive transport [21].

The effects of inertial resistance can be observed in the response of an initially stationary gas to a sudden change of pressure at a boundary of a one-dimensional porous bed. A suitable dimensionless pressure, varying between zero and one, is

$$P \equiv \frac{p - p_0}{p_1 - p_0} \tag{12}$$

p_0 is the ambient pressure while p_1 is the applied pressure.

A dimensionless position is expressed as a fraction of the bed length L.

$$X \equiv \frac{x}{L} \tag{13}$$

The distance is measured from the inlet boundary where the pressure p_1 is applied.

Dimensionless time, in terms of these and previously defined properties, is

$$\tau = \frac{k(p_1 - p_0)\, t}{\mu\, \varepsilon\, L^2} \tag{14}$$

A low Reynolds number flow has a response time corresponding to τ of order unity. Permeability and porosity are presumed uniform.

A dimensionless speed, defined by

$$U \equiv \frac{\mu L u}{k(p_1 - p_0)} \tag{15}$$

expresses the ratio of the local velocity to the velocity that would be observed in an incompressible Darcy flow having the same applied pressure.

For convenience, we refer to the ratio of applied pressure to initial pressure by

$$N \equiv \frac{p_1}{p_0} \tag{16}$$

A Reynolds number characterizing the flow and expressing the importance of deviations from Darcy behavior is

$$Re = \frac{\rho_0 k(p_1 - p_0) b}{\mu L} \tag{17}$$

This is roughly a Reynolds number based on initial density, Darcy velocity and a pore dimension.

In terms of these parameters, Eqs. (10) and (11) become

$$U + Re\ [(N - 1)\ P + 1]\ |U|\ U = -\frac{\partial P}{\partial X} \tag{18}$$

and

$$\frac{\partial P}{\partial \tau} + \frac{\partial}{\partial X}\left[\left(P + \frac{1}{N - 1}\right) U\right] = 0 \tag{19}$$

CHANGE OF SCALE

The dimensionless variables as selected are suitable for description of low Reynolds number flow with large pressure ratio. Under other conditions, a change of time scale is advisable.

Consider first the Darcy flow described by Eqs. (18) and (19) with Re set equal to zero. Substitution yields the single differential equation describing the pressure

$$\frac{\partial P}{\partial \tau} = \frac{1}{2} \frac{\partial^2}{\partial X^2} \left(P^2 + \frac{2P}{N - 1} \right) \tag{20}$$

When the pressure ratio is well in excess of one, gas in the Darcy flow regime will respond to changes in a time τ of order unity. Darcy flow in a finite bed will approach steady state in a time of this magnitude.

For very large Reynolds number, however, the inertial resistance dominates. Consider, for simplicity, flow in the positive X direction so that the absolute value $|U|$ becomes U and the pressure gradient is negative. In this case and for large Re, Eq. (18) reduces to

$$U^2 = \frac{- \frac{\partial P}{\partial X}}{Re \left[(N - 1) P + 1 \right]} \tag{21}$$

and the pressure is governed by

$$\left[Re \ (N - 1) \right]^{1/2} \frac{\partial P}{\partial \tau} + \frac{\partial}{\partial X} \left[- \frac{1}{2} \frac{\partial}{\partial X} \left(P^2 + \frac{2P}{N - 1} \right) \right]^{1/2} = 0 \tag{22}$$

Now, when N is large, the appropriate time scale is seen to be

$$T \equiv \frac{\tau}{\left[Re \ (N - 1) \right]^{1/2}} = \left(\frac{k \, p_o}{\rho_o \, \varepsilon^2 \, L^3 b \, \mu} \right)^{1/2} t \tag{23}$$

so that the pressure obeys

$$\frac{\partial P}{\partial T} + \frac{\partial}{\partial X} \left[- \frac{1}{2} \frac{\partial}{\partial X} \left(P^2 + \frac{2P}{N - 1} \right) \right]^{1/2} = 0 \tag{24}$$

For small pressure ratio, examination of Eq. (20) reveals that the suitable time scale for Darcy flow is

$$\frac{\tau}{N-1} = \frac{k\, p_o\, t}{\mu\, \varepsilon\, L^2} \tag{25}$$

while, for high Reynolds number and small pressure ratio, rearranging Eq. (24) indicates that a time scale

$$\frac{T}{(N-1)^{1/2}} = \frac{\tau}{(N-1)(Re)^{1/2}} = \left[\frac{k\, p_o}{\rho_o\, \varepsilon^2\, L^3\, b\, \mu\, (N-1)}\right]^{1/2} t \tag{26}$$

should be employed.

Choice of an appropriate time scale is important in numerical calculations. Without consideration of the relaxation time, finite difference time steps are not well chosen. Excessively large time steps result in loss of accuracy while calculations using overly small time steps are inefficient.

SIMILARITY ANALYSES

While our primary interest is in flow in finite beds, it is worthwhile to consider the flow into a semi-infinite bed. There are several reasons for this interest. The short time behavior of flow in a finite bed is well approximated by flow in a semi-infinite bed. Additionally, under certain conditions to be described, the transient pressure in a semi-infinite bed depends only on a single variable and not on position and time separately. Such a flow is said to be similar.

Similarity permits several general conclusions about early time behavior and also permits one to assess the accuracy of numerical solutions. This latter feature is particularly valuable when, as is the case here, the governing equations are nonlinear and exact solutions for comparison do not exist.

Consider a flow into a semi-infinite bed. The gas in the bed is initially stationary and at ambient pressure. The pressure at the surface is suddenly increased to some high constant value. The flow then is governed by Eqs. (18) and (19) subject to

$$\begin{aligned} P &= 0 \quad \text{at} \quad \tau = 0 \\ P &= 1 \quad \text{at} \quad X = 0 \\ P &\to 0 \quad \text{as} \quad X \to \infty \end{aligned} \tag{27}$$

For Darcy flow, governed by Eq. (20) and subject to these conditions, the pressure has been shown [19] to be similar. The pressure depends only on a single variable defined by

$$\theta = \frac{X}{2(\tau)^{1/2}} = \frac{x}{2}\sqrt{\frac{\varepsilon\mu}{k(p_1 - p_o)\, t}} \tag{28}$$

since both the differential equation and boundary conditions can be written in terms of θ alone. Equation (20) is

$$4\theta \frac{dP}{d\theta} + \frac{d^2}{d\theta^2}\left(P^2 + \frac{2P}{N-1}\right) = 0 \tag{29}$$

and conditions (27) become

$$\begin{aligned} P &= 1 \quad \text{at} \quad \theta = 0 \\ P &\to 0 \quad \text{as} \quad \theta \to \infty \end{aligned} \tag{30}$$

Note that θ does not contain a length scale L.

The pressure distribution for this Darcy gas flow in a semi-infinite bed was calculated by Morrison [19] and the results are shown in Fig. 1. Several values of pressure ratio have been selected. The Reynolds number is zero in each of these cases.

For high Reynolds number flow, we may also demonstrate similarity. The similarity variable is different however from the variable, θ, that has been used for the low Reynolds number flow. Consider the flow governed by Eq. (24) and subject to the conditions (27). If we define

$$\xi = \frac{X}{T^{2/3}} \tag{31}$$

then Eq. (24) can be written as the ordinary differential equation

$$\xi \frac{dP}{d\xi} - \frac{d}{d\xi}\left[\frac{-9}{8}\frac{d}{d\xi}\left(P^2 + \frac{2P}{N-1}\right)\right]^{1/2} = 0 \tag{32}$$

and conditions (27) are expressed in terms of ξ by

$$\begin{aligned} P &= 1 \quad \text{at} \quad \xi = 0 \\ P &\to 0 \quad \text{as} \quad \xi \to \infty \end{aligned} \tag{33}$$

corresponding to the conditions (30) applied to Darcy flow. ξ, like θ, contains no length L.

The high Reynolds number gas flow resulting from a step change in surface

pressure has been shown to be similar. The pressure depends only on ξ. The short time flow in a finite column will behave in this manner. This similarity requirement can be used to judge the accuracy of finite difference calculations. Such calculations are performed and displayed in similar form in the section on results of calculations.

NUMERICAL TECHNIQUE

A numerical procedure has been developed for the solution of Eqs. (18) and (19) governing the transient non-Darcy isothermal gas flow in one dimension. Because stability considerations may severely restrict the allowable time step in an explicit calculation, an implicit method was developed.

Explicit methods have been developed, e.g. [22-26], that are unconditionally stable for solution of the linear diffusion equation. It remains to evaluate the applicability of their analogs to the nonlinear set of equations treated here. Consistency requirements will, at least in certain cases, place limits on the allowable step sizes.

A uniform mesh is employed. The node spacing in the X direction is ΔX and the spatial index is i. The temporal step size is $\Delta\tau$ and the time level is denoted by the superscript k.

Suitable finite difference expressions for the derivatives may now be developed. For this purpose, it is useful to interpret P_i as the dimensionless pressure at node i and U_i as the dimensionless velocity midway between nodes i and i + 1. The spatial derivative in Eq. (19) expresses the rate of mass flow into a spatial element. At node i, the derivative is approximated by

$$\frac{\partial}{\partial X}\left[\left(P + \frac{1}{N-1}\right)U\right] \approx \frac{1}{2\Delta X}\left[\left(P_{i+1} + P_i + \frac{2}{N-1}\right)U_i - \left(P_i + P_{i-1} + \frac{2}{N-1}\right)U_{i-1}\right] \tag{34}$$

The velocities in this expression may be expressed using a finite difference equivalent of Eq. (18).

$$U_i = \frac{-1}{\Delta X}\,\frac{P_{i+1} - P_i}{1 + \dfrac{(N-1)\,Re}{2}\left(P_{i+1} + P_i + \dfrac{2}{N-1}\right)|U_i|} \tag{35}$$

The pressure gradient of Eq. (18) has been replaced by a central difference approximation for the derivative midway between i and i + 1.

The finite difference approximation of Eq. (19) is formed using a forward difference in time and expressing the spatial derivative as a weighted average of finite difference expressions at the k and k + 1 levels. Using Eqs. (34) and (35), we have

$$\frac{P_i^{k+1} - P_i}{\Delta\tau} = \frac{1}{2(\Delta X)^2}\left\{\beta\left[\frac{\left(P_{i+1} + P_i + \frac{2}{N-1}\right)(P_{i+1} - P_i)}{1 + \frac{(N-1)\,Re}{2}\left(P_{i+1} + P_i + \frac{2}{N-1}\right)|U_i|}\right.\right.$$

$$\left.\left. - \frac{\left(P_i + P_{i-1} + \frac{2}{N-1}\right)(P_i - P_{i-1})}{1 + \frac{(N-1)\,Re}{2}\left(P_i + P_{i-1} + \frac{2}{N-1}\right)|U_{i-1}|}\right]^{k+1}\right. \tag{36}$$

$$\left. + (1-\beta)\left[\left(P_{i+1} + P_i + \frac{2}{N-1}\right)U_i - \left(P_i + P_{i-1} + \frac{2}{N-1}\right)U_{i-1}\right]^{k}\right\}$$

The spatial derivative is expressed differently at the two time levels for reasons that will shortly be apparent. β is the weighting factor. It can assume values between 0 and 1. β equal to zero corresponds to an explicit formulation. β greater than zero is implicit. By analogy with the linear diffusion equation, β greater than or equal to 1/2 can be expected to yield stable results, independent of time step. In the absence of rigorous stability limits for nonlinear equations, such analogs provide useful guidance. The corresponding finite different approximation, with β equal to 1/2, is the Crank-Nicolson method [27]. The Crank-Nicolson method has a truncation error of $(\Delta\tau)^2$, $(\Delta X)^2$. When β

is not equal to 1/2, the truncation error is of order $\Delta\tau$, $(\Delta X)^2$. For the nonlinear equation treated here, β equal to 1/2 would not yield higher order error so that the choice of β is somewhat arbitrary. β equal to 1/2 has been satisfactory in applications to date; however, the option of increasing β is retained.

The nonlinear diffusion equation governing Darcy flow of a gas has been solved, using β equal to 1/2, by Bruce, Peaceman, Rachford, and Rice [28]. This procedure is efficient, iterative, and stable. It has been widely employed.

Defining

$$h = \frac{(\Delta X)^2}{\Delta \tau} \tag{37}$$

and rearranging with the unknowns, the variables at the k + 1 time level, on the left and known quantities, those evaluated at the k time level, on the right.

$$4h\, P_i^{k+1} - 2\beta\left[\frac{\left(P_{i+1} + P_i + \frac{2}{N-1}\right)(P_{i+1} - P_i)}{1 + \frac{(N-1)\,Re}{2}\left(P_{i+1} + P_i + \frac{2}{N-1}\right)|U_i|} - \frac{\left(P_i + P_{i-1} + \frac{2}{N-1}\right)(P_i - P_{i-1})}{1 + \frac{(N-1)\,Re}{2}\left(P_i + P_{i-1} + \frac{2}{N-1}\right)|U_{i-1}|}\right]^{k+1} = \tag{38}$$

$$4h\, P_i^k + 2(1-\beta)\left[\left(P_{i+1} + P_i + \frac{2}{N-1}\right)U_i - \left(P_i + P_{i-1} + \frac{2}{N-1}\right)U_{i-1}\right]^k$$

This relation, to be solved for the pressures at the new time level, is nonlinear in the unknowns. The pressures are obtained by linearization and iterative solution of the resulting set of linear equations. The nonlinear portion is factored and then linearized by assuming a value for part of the expression. Because the assumed value may not be presumed correct, an iterative procedure is employed to generate progressively better assumptions.

Using the superscript K + 1 to denote assumed values at level k + 1, Eq. (38) is linearized in a manner consistent with, but generalizing, the linearization of Bruce, Peaceman, Rachford, and Rice.

$$4h\,P_i^{k+1} - 2\beta\left[\frac{P_{i+1} + P_i + \frac{2}{N-1}}{1 + \frac{(N-1)\,Re}{2}\left(P_{i+1} + P_i + \frac{2}{N-1}\right)|U_i|}\right]^{K+1}(P_{i+1} - P_i)^{k+1}$$

$$+ 2\beta\left[\frac{P_i + P_{i-1} + \frac{2}{N-1}}{1 + \frac{(N-1)\,Re}{2}\left(P_i + P_{i-1} + \frac{2}{N-1}\right)|U_{i-1}|}\right]^{K+1}(P_i - P_{i-1})^{k+1}$$

$$= 4h\,P_i^k + 2(1-\beta)\left[\left(P_{i+1} + P_i + \frac{2}{N-1}\right)U_i - \left(P_i + P_{i-1} + \frac{2}{N-1}\right)U_{i-1}\right]^k \tag{39}$$

We have a set of linear equations among the unknown pressures. In a more compact notation, this is

$$A_i\,P_{i-1}^{k+1} + B_i\,P_i^{k+1} + C_i\,P_{i+1}^{k+1} = D_i \tag{40}$$

where

$$A_i = -2\beta\left[\frac{P_{i+1} + P_i + \frac{2}{N-1}}{1 + \frac{(N-1)\,Re}{2}\left(P_{i+1} + P_i + \frac{2}{N-1}\right)|U_i|}\right]^{K+1} \tag{41}$$

$$C_i = -2\beta\left[\frac{P_i + P_{i-1} + \frac{2}{N-1}}{1 + \frac{(N-1)\,Re}{2}\left(P_i + P_{i-1} + \frac{2}{N-1}\right)|U_{i-1}|}\right]^{K+1} \tag{42}$$

$$B_i = 4h - A_i - C_i \tag{43}$$

$$D_i = 4h\,P_i^k + 2(1-\beta)\left[\left(P_{i+1} + P_i + \frac{2}{N-1}\right)U_i - \left(P_i + P_{i-1} + \frac{2}{N-1}\right)U_{i-1}\right]^k \tag{44}$$

The set of finite difference equations (40) has a tridiagonal coefficient matrix and thus the iterations can be done efficiently. The solution of a set of n such equations can be obtained using a well known algorithm, described by Bruce, Peaceman, Rachford, and Rice [28], requiring only 5n - 2 storage locations and using a number of operations of order n.

If β is chosen equal to zero, the pressures are uncoupled, the formulation is simpler, the method is explicit but stability requirements restrict the temporal step size $\Delta\tau$ to the order of $(\Delta X)^2$. Within this restriction, the explicit formulation has also been successfully used by the author. The restriction vanishes when β greater than 1/2 is used.

RESULTS OF CALCULATIONS

A series of calculations have been performed using the implicit procedure just described. Transient response characteristics are examined by considering the flow produced by a step change in pressure at one end of a finite bed. The other end remains open to the atmosphere, its pressure unchanged. The flow, then, is governed by Eqs. (18) and (19) subject to

$$\begin{aligned} P &= 0 \quad \text{at} \quad \tau = 0 \\ P &= 1 \quad \text{at} \quad X = 0 \\ P &= 0 \quad \text{at} \quad X = 1 \end{aligned} \tag{45}$$

Only the pressure ratio N, defined by Eq. (16), and the Reynolds number Re, defined by Eq. (17), need be specified to describe the flow.

Consider a pressure ratio of 50. The flow was analyzed for several values of Re in order to display the effects of gas inertia. In Figs. 2, 3, and 4, results are presented for selected values of the dimensionless time τ.

Figure 2 shows flow at zero Reynolds number, Darcy flow. For the largest time selected, τ equal to 3.0, the pressure distribution is, for all practical purposes, fully developed. Calculated pressures at τ equal to 3.0 agree with those at τ equal to 2.5 to at least five digits. The flow can be considered to be in a steady state. For short times, τ less than about 0.38, the effect of the distant boundary on the Darcy flow is negligible. The gas moves as if through a semi-infinite bed. The short time flow is similar. The similarity variable is θ and the early pressure history is very well described by the infinite pressure ratio curve of Fig. 1.

Figures 3 and 4 reveal how increasing Reynolds number affects this behavior. Because of the added inertial resistance, the response is not as rapid. Neither of these flows is fully developed by τ equal to 3. At

least for the flow having a Reynolds number of 10, the time scale T, defined by Eq. (23), is more useful.

Changing scales, we will again describe the Re equal to 10, N equal to 50 flow. For selected values of the dimensionless time T, the pressure distribution is presented in Fig. 5. The full range of the flow response is observed within a range of T of order unity. In addition, and of greater importance, all flows possessing large Re and large N, and subject to conditions (45), are virtually indistinguishable from the flow presented in Fig. 5. In this high Re, high N range, the pressure distribution is nearly independent of Re and N when presented as a function of X and T.

The curve for T equal to 3.0 does not correspond to steady state. Only for much larger time is steady state achieved. This steady state pressure distribution is independent of Reynolds number and the final distribution corresponds to the τ equal to 3.0 curve of Fig. 2. The independence of the steady distribution from Reynolds number follows from Eqs. (18) and (19) with the temporal derivative set equal to zero. A non-Darcy flow resistance relation other than Forchheimer's relation would not necessarily yield this result.

For times prior to significant pressure change at X equal to 1, this high Re, high N flow is nearly similar. It behaves as flow in a semi-infinite porous medium. The appropriate similarity variable is ξ, defined by Eq. (31) and describing the high Reynolds number flow governed by Eq. (32).

Results of calculations for very large Re and N are shown in similar form in Fig. 6. All the curves of Fig. 4 as well as the short time curves of Figs. 3 and 5 are well represented by this single curve.

CONCLUSIONS

Non-Darcy flow of an ideal gas has been investigated. Relations governing transient isothermal flow in one dimension were considered. Pressures resulting from a step change in pressure at the boundary of a semi-infinite bed were shown to depend on a single variable for high Reynolds number flow. A numerical technique was developed to describe transient flows in finite beds. Results have been obtained and presented showing response characteristics of non-Darcy flows.

CAPTIONS FOR FIGURES

Figure 1 Pressure distribution in an infinite bed, low Reynolds number [19]

Figure 2 Pressure distribution in a finite bed, low Reynolds number

Figure 3 Pressure distribution in a finite bed, intermediate Reynolds number

Figure 4 Pressure distribution in a finite bed, high Reynolds number

Figure 5 Pressure distribution in a finite bed, high Reynolds number

Figure 6 Pressure distribution in an infinite bed, high Reynolds number

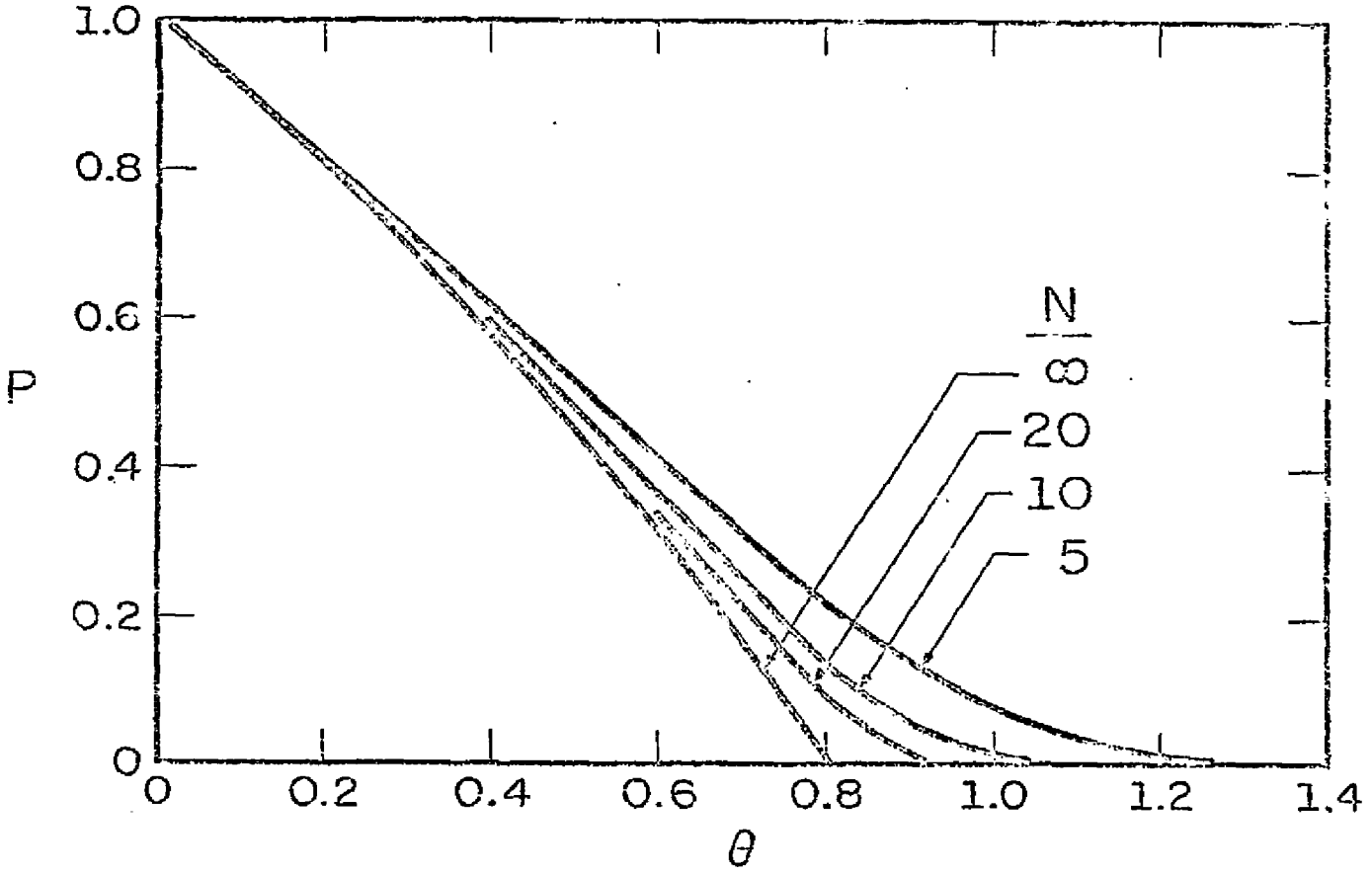

Figure 1 Pressure distribution in an infinite bed, low Reynolds number [19]

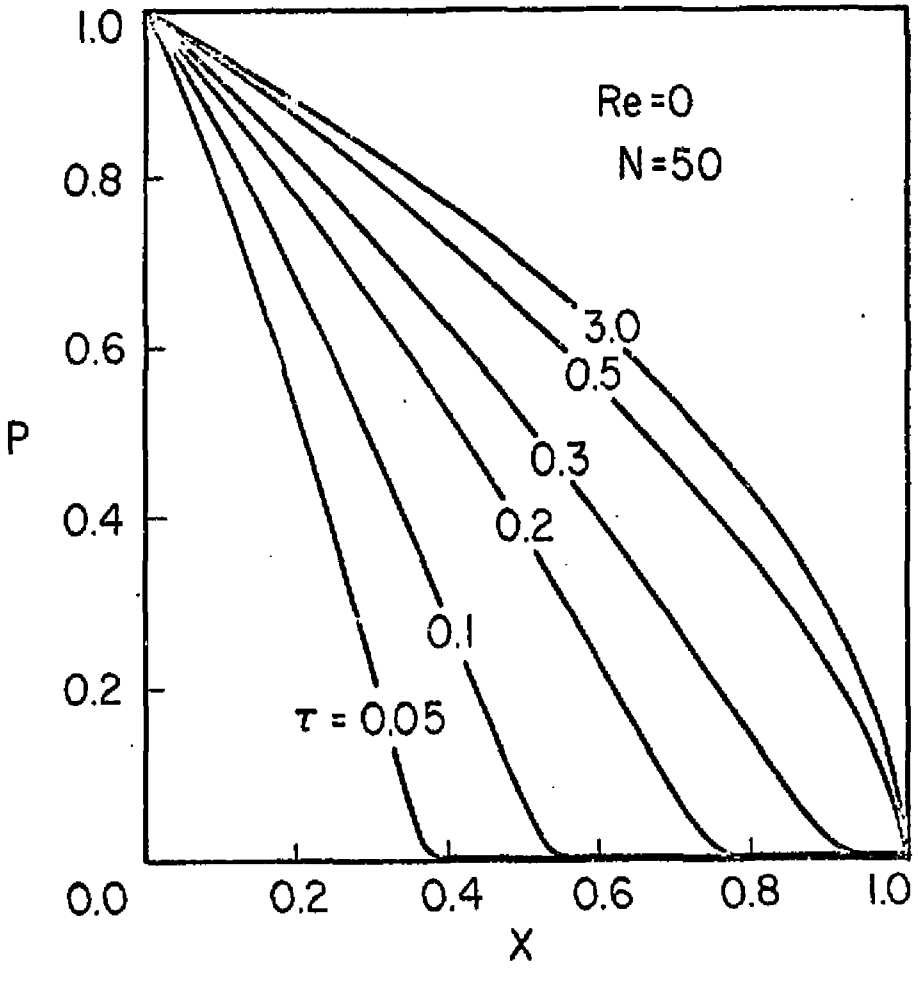

Figure 2 Pressure distribution in a finite bed, low Reynolds number

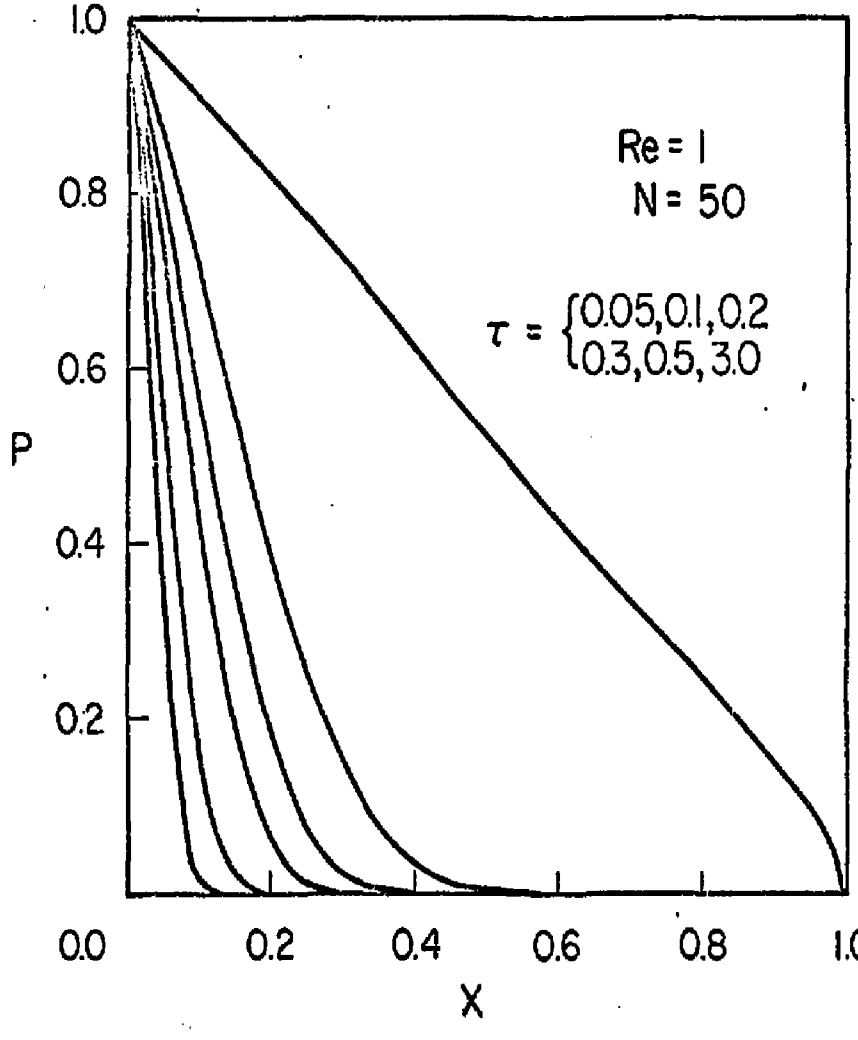

Figure 5 Pressure distribution in a finite bed, intermediate Reynolds number

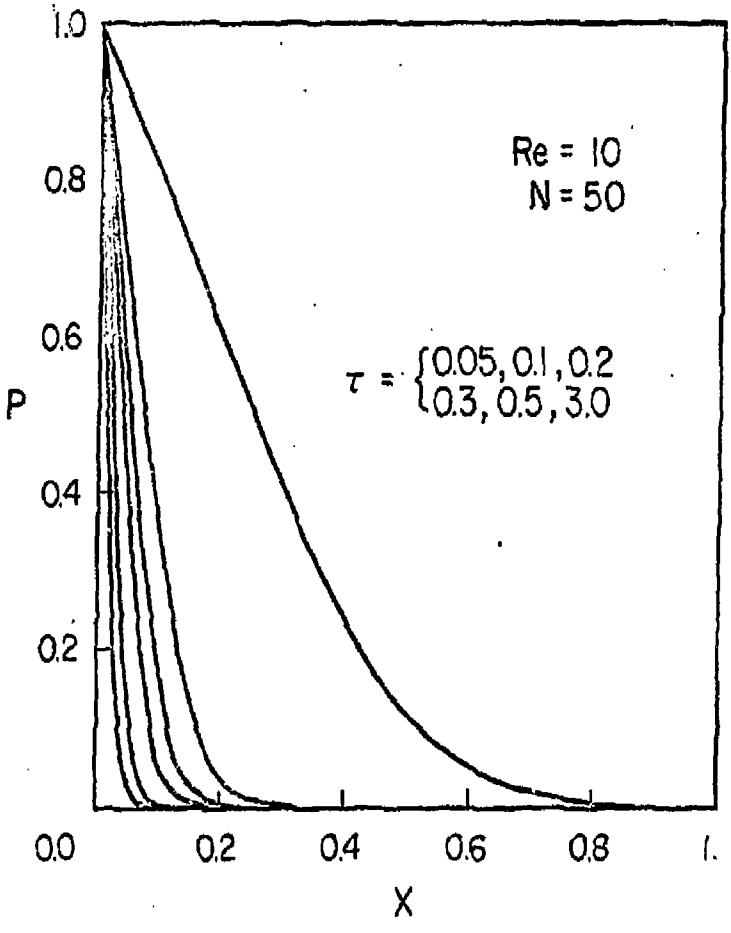

Figure 4 Pressure distribution in a finite bed, high Reynolds number

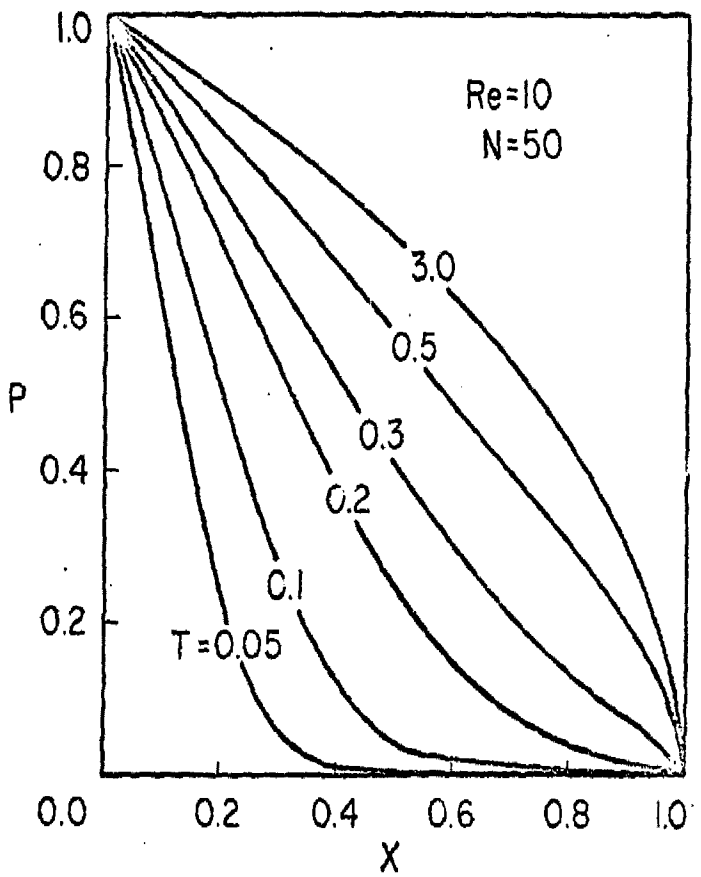

Figure 5 Pressure distribution in a finite bed, high Reynolds number

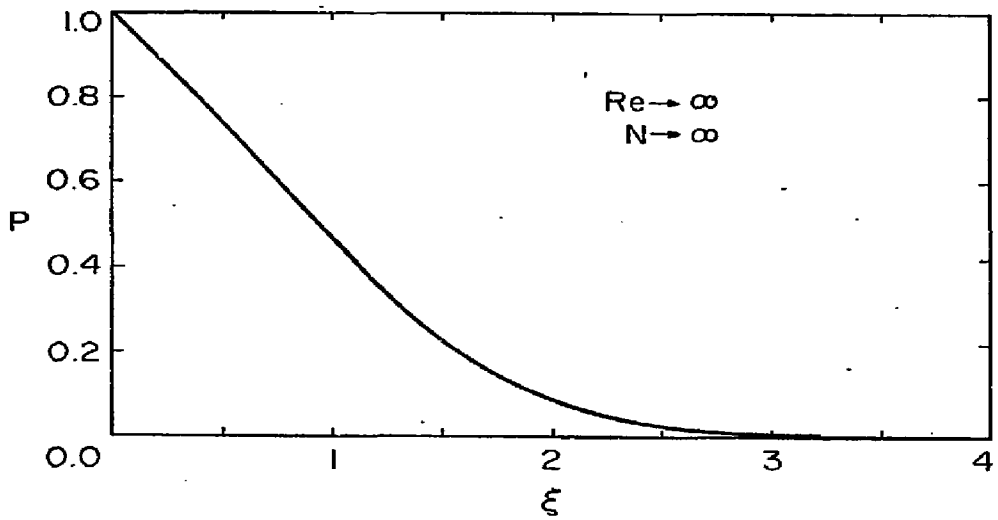

Figure 6 Pressure distribution in an infinite bed, high Reynolds number

REFERENCES

1. Forchheimer, Ph.: "Wasserbewegung durch Boden", Zeitschrift des Vereines Deutscher Ingenieure (1901) vol. 45, 1781-1788.

2. Carman, P. C.: Flow of Gases through Porous Media, Academic Press, N.Y. (1956).

3. Happel, J.: "Viscous Flow in Multiparticle Systems: Slow Motion of Fluids Relative to Beds of Spherical Particles", A.I.Ch.E.J. (1958) vol. 4, 197-201.

   Happel, J.: "Fluid Flow in Multiparticle Systems", Trans. N.Y. Acad. Sci. (1958) vol. 20, 404-410.

4. Burke, S. P. and Plummer, W.B.: "Gas Flow through Packed Columns", Ind. Eng. Chem. (1928) vol. 20, 1196-1200.

5. Ergun, S. and Orning, A. A.: "Fluid Flow through Randomly Packed Columns and Fluidized Beds", Ind. Eng. Chem. (1949) vol. 41, 1179-1184.

6. Green, L., Jr., and Duwez, P.: "Fluid Flow through Porous Metals", J. Appl. Mech. (1951) vol. 18, 39-45.

7. Ergun, S.: "Fluid Flow through Packed Column", Chem. Eng. Prog. (1952) vol. 48, 89-94.

8. Schneebeli, G.: "Experiences sur la limite de validité de la loi de Darcy et l'apparition de la turbulence dans un écoulement de filtration", La Houille Blanche (1955) vol. 10, 141-149.

9. Ward, J.: "Turbulent Flow in Porous Media", J. Hydraulics Div. A.S.C.E. (1964) vol. 90, HY5, 1-12.

10. Irmay, S.: "On the Theoretical Derivation of Darcy and Forchheimer Formulas", Trans., AGU (1958) Vol. 39, 702-707.

11. Bachmat, Y.: "Basic Transport Coefficients as Aquifer Characteristics", I.A.S.H. Symp. Hydrology of Fractured Rocks, Dubrovnik (1965) vol. 1, 63-75.

12. Blick, E. F.,: "Capillary-Orifice Model for High-Speed Flow through Porous Media", I.&E.C. Process Design and Development (1966) vol. 5, 90-94.

13. Polubarinova-Kochina, P. Ya.: Theory of Ground Water Movement, Princeton University Press, Princeton, N.J. (1962).

14. Beavers, G. S. and Sparrow, E. M.: "Compressible Gas Flow through a Porous Material", Int. J. Heat Mass Transfer (1971) vol. 14, 1855-1859.

15. Masha, B. A., Beavers, G. S., and Sparrow, E. M.: "Experiments on the Resistance Law for Non-Darcy Compressible Gas Flows in Porous Media", J. Fluids Engr., Trans., ASME (1974) vol. 96, 353-357.

16. Swift, G. W. and Kiel, O. G.: "The Prediction of Gas-Well Performance Including the Effect of Non-Darcy Flow", Trans., AIME (1962) vol. 225, 791-798.

17. Rowan, G. and Clegg, M. W.: "An Approximate Method for Non-Darcy Radial Gas Flow", Trans., AIME (1964) vol. 231, 96-114.

18. Dranchuk, P. M. and Chwyl, E.: "Transient Gas Flow through Finite Linear Porous Media", J. Can. Pet. Tech. (1969) vol. 8, 57-65.

19. Morrison, F. A., Jr.: "Transient Gas Flow in a Porous Column," I.&E.C. Fundamentals (1972) vol. 11, 191-197.

20. Morrison, F. A., Jr.: "Transient Multiphase Multicomponent Flow in Porous Media", Int. J. Heat Mass Transfer (1975) vol. 16, 2331-2342.

21. Downing, R. S. and Morrison, F. A., Jr.: "Convective and Dispersive Transport in a Porous Medium", to appear.

22. DuFort, E. C. and Frankel, S. P.: "Stability Considerations in the Numerical Treatment of Parabolic Differential Equations", Math. Tables Aids Comput. (1953) vol. 7, 135-152.

23. Saul'ev, V. K.: "A Method of Numerical Solution for the Diffusion Equation", Dokl. Akad. Nauk SSSR (1957) vol. 115, 1077-1079.

24. Larkin, B. K.: "Some Stable Explicit Difference Approximations to the Diffusion Equation", Math. of Comput. (1964) vol. 18, 196-202.

25. Barakat, H. Z. and Clark, J. A.: "On the Solution of the Diffusion Equations by Numerical Methods", J. Heat Transfer, Trans. ASME (1966) vol. 88, 421-427.

26. Liu, S.-L.: "Stable Explicit Difference Approximations to Parabolic Partial Differential Equations", A.I.Ch.E.J. (1969) vol. 15, 334-338.

27. Crank, J. and Nicolson, P.: "A Practical Method for Numerical Evaluation of Solutions of Partial Differential Equations of the Heat Conduction Type", Proc. Camb. Phil. Soc. (1947) vol. 43, 50-67.

28. Bruce, G. H., Peaceman, D. W., Rachford, H. H., Jr., and Rice, J. D.: "Calculations of Unsteady-State Gas Flow through Porous Media", Trans., AIME (1953) vol. 198, 79-92.